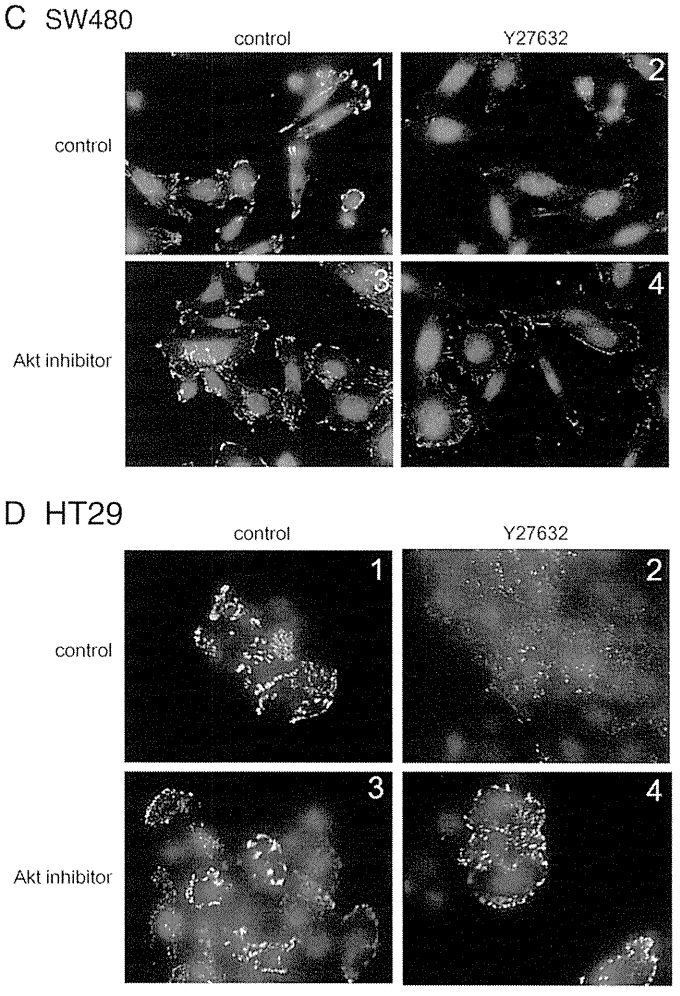

Fig. 4 (*continued*).

with Y27632 (Fig. 4C, panel 4 compared to panel 2). Similarly, we observed that the Akt inhibitor significantly restored the loss of focal adhesion induced by Y27632 in HT29 cells (Fig. 4D). These results suggest that the alteration of focal adhesion formation induced by Y27632 is mediated through the Akt pathway in colon cancer cells.

4. Discussion

Because metastasis is common among many types of cancer, and is related to the prognosis of most cancers, researchers have expanded their interests into the anti-invasive and anti-angiogenic compounds that do not directly to kill tumor cells, such as matrix metalloproteinase (MMP) inhibitors or anti-vascular endothelial growth factor (VEGF) antibodies (Egeblad and Werb, 2002; Kerbel and Folkman, 2002). In the present study, we investigated the role of Rho-kinase in the migration of SW480 colon cancer cells. We have recently reported that Rho-kinase negatively regulates EGF-induced cell proliferation at a point upstream of Akt/GSK-3β in colon cancer cells (Nakashima et al., 2010). EGF-induced phosphorylation of Akt and GSK-3β, and the subsequent increase in the phosphorylation of the retinoblastoma tumor suppressor protein, as well as an increase in the cyclin D1 protein expression level, were dose-dependently enhanced when the cells were pretreated with Y27632 (Nakashima et al., 2010). In this study, we found that the inhibition of Rho-kinase caused an increase in cell migration (Fig. 1), thus suggesting that Rho-kinase is involved not only in cell cycle progression, but also in the migration of colon cancer cells.

VEGF has been previously shown to induce the migration of colon cancer cells (Diaz-Rubio, 2006). Although SW480 cells can produce VEGF (Fig. 2A), the cell migration induced by Y27632 was not due to an increase in VEGF release from SW480 cells (Fig. 2A), thus indicating that Rho-kinase is not involved in the process of VEGF release. Moreover, it has recently been suggested that VEGF has both a positive and a negative regulatory effect on tumor growth (Vecchiarelli-Federico et al., 2010). Although we showed that Rho-kinase was strongly activated at baseline in our colon cancer cell line, we speculate that VEGF released in an autocrine manner from SW480 cells might regulate the migration of these cells via suppression of Rho-kinase.

We next performed an immunofluorescence microscopy study to observe the effect of Y27632 on the localization of focal adhesion molecules, such as vinculin, caveolin-1 and tyrosine-phosphorylated proteins (Fig. 3). We thus showed that Y27632 caused a marked loss in the size and number of focal adhesions around the cell periphery, as revealed by vinculin staining (Fig. 3, panel 2 compared to panel 1). Staining with antibodies against phosphorylated caveolin-1 and phosphotyrosine showed similar results (Fig. 3, panels 3–6). These findings strongly suggest that the inhibition of Rho-kinase causes the marked decrease in the formation of the focal adhesion complex, indicating that Rho-kinase negatively regulates colon cancer cell migration.

We further examined the mechanism underlying Y27632-induced cell migration in colon cancer cells. We first found that Y27632 induced the activation of Akt and GSK-3β (Fig. 4). We also observed that Y27632 failed to affect the phosphorylation of p44/p42 mitogen-activated protein kinase (MAPK), p38 MAPK and stress-activated protein kinase/c-*Jun* N-terminal kinase (data not shown). Y27632-induced activation of Akt was suppressed by pretreatment with an Akt-specific inhibitor (Fig. 4B). Interestingly, we demonstrated the Y27632-induced loss of the localization of vinculin to be restored when the cells were pretreated with the Akt inhibitor (Fig. 4C), thus suggesting that Rho-kinase negatively regulates the formation of focal adhesion via the Akt pathway in colon cancer cells. Moreover, we observed similar results in HT29 cells (Fig. 4D), thus suggesting that these results are not confined to a specific cell line. A schematic representation of the involvement of Rho-kinase in the migration of colon cancer cells is shown in Fig. 5.

The Rho/Rho-kinase pathway takes part in cancer progression by regulating actin cytoskeleton reorganization. Since a specific Rho-kinase inhibitor was found to suppress tumor growth and metastasis (Itoh et al., 1999), it has been reported that the Rho/Rho-kinase pathway may become a molecular target for the prevention of cancer invasion and metastasis. In contrast, a recent study showed the

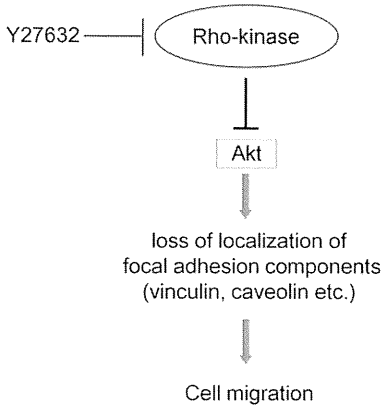

Fig. 5. A schematic representation of the involvement of Rho-kinase in the migration of colon cancer cells. In unstimulated colon cancer cells, Rho-kinase is generally activated at baseline, and suppresses the activation of Akt, which induces the loss of localization of focal adhesion components (vinculin, caveolin, etc.) and leads to cell migration. Therefore, the inhibition of Rho-kinase by Y27632 causes activation of Akt, indicating that Rho-kinase negatively regulates the migration of colon cancer cells.

activation of Rho-kinase to lead to an inhibition of motility in human breast cancer cells (Brew et al., 2009). In this report, indole-3-carbinol (I3C), a phytochemical derived from cruciferous vegetables, was shown to decrease metastatic spread of tumors in experimental animals, and I3C induced stress fibers and peripheral focal adhesions in a Rho-kinase-dependent manner (Brew et al., 2009). In addition, Y27632, a specific Rho-kinase inhibitor, reportedly interferes with Ras-mediated transformation, and constitutively active form of mutant Rho-kinase collaborate with activated Raf in transformation assays in NIH3T3 fibroblastic cells (Sahai et al., 1999). On the other hand, the inactivation of the Rho/Rho-kinase pathway has been shown to promote oncogenic Ras-induced transformation in Rat1 fibroblast cells (Izawa et al., 1998), thus suggesting Rho-kinase to play a negative role in oncogenic cells which is consistent with our previous study (Nakashima et al., 2010). Although we demonstrated that Rho-kinase regulates not only cell cycle progression (Nakashima et al., 2010), but also cell migration in colon cancer cells, further investigations are therefore required to clarify the precise role of Rho-kinase in cancer metastasis.

In conclusion, Rho-kinase negatively regulates cell migration at a point upstream of Akt/GSK-3β in colon cancer cells. This is the first report to show that Rho-kinase is involved in the negative regulation of colon cancer cell migration, thus providing important insight into the future development of potential therapeutic approaches for colon cancer patients. In other words, the regulation of Rho-kinase might be considered to be a new clinical target for cancer management, including the management of colon cancer.

Acknowledgments

We are very grateful to Ms. Yoko Kawamura for her skillful technical assistance. This work was supported in part by a Grant-in-Aid for Scientific Research (No. 22790639 to S.A.) from the Ministry of Education, Science, Sports and Culture of Japan.

References

Adachi, S., Nagao, T., Ingolfsson, H.I., Maxfield, F.R., Andersen, O.S., Kopelovich, L., Weinstein, I.B., 2007. The inhibitory effect of (−)-epigallocatechin gallate on activation of the epidermal growth factor receptor is associated with altered lipid order in HT29 colon cancer cells. Cancer Res. 67, 6493–6501.

Adachi, S., Nagao, T., To, S., Joe, A.K., Shimizu, M., Matsushima-Nishiwaki, R., Kozawa, O., Moriwaki, H., Maxfield, F.R., Weinstein, I.B., 2008. (−)-Epigallocatechin gallate causes internalization of the epidermal growth factor receptor in human colon cancer cells. Carcinogenesis 29, 1986–1993.

Adachi, S., Natsume, H., Yamauchi, J., Matsushima-Nishiwaki, R., Joe, A.K., Moriwaki, H., Kozawa, O., 2009a. p38 MAP kinase controls EGF receptor downregulation via phosphorylation at Ser1046/1047. Cancer Lett. 277, 108–113.

Adachi, S., Shimizu, M., Shirakami, Y., Yamauchi, J., Natsume, H., Matsushima-Nishiwaki, R., To, S., Weinstein, I.B., Moriwaki, H., Kozawa, O., 2009b. (−)-Epigallocatechin gallate downregulates EGF receptor via phosphorylation at Ser1046/1047 by p38 MAPK in colon cancer cells. Carcinogenesis 30, 1544–1552.

Bar-Sagi, D., Hall, A., 2000. Ras and Rho GTPases: a family reunion. Cell 103, 227–238.

Brew, C.T., Aronchik, I., Kosco, K., McCammon, J., Bjeldanes, L.F., Firestone, G.L., 2009. Indole-3-carbinol inhibits MDA-MB-231 breast cancer cell motility and induces stress fibers and focal adhesion formation by activation of Rho kinase activity. Int. J. Cancer 124, 2294–2302.

Burridge, K., 1981. Are stress fibres contractile? Nature 294, 691–692.

Burridge, K., Chrzanowska-Wodnicka, M., 1996. Focal adhesions, contractility, and signaling. Annu. Rev. Cell Dev. Biol. 12, 463–518.

Cross, D.A., Alessi, D.R., Cohen, P., Andjelkovich, M., Hemmings, B.A., 1995. Inhibition of glycogen synthase kinase-3 by insulin mediated by protein kinase B. Nature 378, 785–789.

Diaz-Rubio, E., 2006. Vascular endothelial growth factor inhibitors in colon cancer. Adv. Exp. Med. Biol. 587, 251–275.

Egeblad, M., Werb, Z., 2002. New functions for the matrix metalloproteinases in cancer progression. Nat. Rev. Cancer 2, 161–174.

Fritz, G., Just, I., Kaina, B., 1999. Rho GTPases are over-expressed in human tumors. Int. J. Cancer 81, 682–687.

Humphries, J.D., Wang, P., Streuli, C., Geiger, B., Humphries, M.J., Ballestrem, C., 2007. Vinculin controls focal adhesion formation by direct interactions with talin and actin. J. Cell Biol. 179, 1043–1057.

Itoh, K., Yoshioka, K., Akedo, H., Uehata, M., Ishizaki, T., Narumiya, S., 1999. An essential part for Rho-associated kinase in the transcellular invasion of tumor cells. Nat. Med. 5, 221–225.

Izawa, I., Amano, M., Chihara, K., Yamamoto, T., Kaibuchi, K., 1998. Possible involvement of the inactivation of the Rho–Rho-kinase pathway in oncogenic Ras-induced transformation. Oncogene 17, 2863–2871.

Joshi, B., Strugnell, S.S., Goetz, J.G., Kojic, L.D., Cox, M.E., Griffith, O.L., Chan, S.K., Jones, S.J., Leung, S.P., Masoudi, H., Leung, S., Wiseman, S.M., Nabi, I.R., 2008. Phosphorylated caveolin-1 regulates Rho/ROCK-dependent focal adhesion dynamics and tumor cell migration and invasion. Cancer Res. 68, 8210–8220.

Kerbel, R., Folkman, J., 2002. Clinical translation of angiogenesis inhibitors. Nat. Rev. Cancer 2, 727–739.

Matsui, T., Amano, M., Yamamoto, T., Chihara, K., Nakafuku, M., Ito, M., Nakano, T., Okawa, K., Iwamatsu, A., Kaibuchi, K., 1996. Rho-associated kinase, a novel serine/threonine kinase, as a putative target for small GTP binding protein Rho. EMBO J. 15, 2208–2216.

McHardy, L.M., Sinotte, R., Troussard, A., Sheldon, C., Church, J., Williams, D.E., Andersen, R.J., Dedhar, S., Roberge, M., Roskelley, C.D., 2004. The tumor invasion inhibitor dihydromotuporamine C activates RHO, remodels stress fibers and focal adhesions, and stimulates sodium-proton exchange. Cancer Res. 64, 1468–1474.

Nakashima, M., Adachi, S., Yasuda, I., Yamauchi, T., Kozawa, O., Moriwaki, H., 2010. Rho-kinase regulates negatively the epidermal growth factor-stimulated colon cancer cell proliferation. Int. J. Oncol. 36, 585–592.

Pellegrin, S., Mellor, H., 2007. Actin stress fibres. J. Cell Sci. 120, 3491–3499.

Pourgholami, M.H., Morris, D.L., 2008. Inhibitors of vascular endothelial growth factor in cancer. Cardiovasc. Hematol. Agents Med. Chem. 6, 343–347.

Ridley, A.J., Schwartz, M.A., Burridge, K., Firtel, R.A., Ginsberg, M.H., Borisy, G., Parsons, J.T., Horwitz, A.R., 2003. Cell migration: integrating signals from front to back. Science 302, 1704–1709.

Riento, K., Ridley, A.J., 2003. Rocks: multifunctional kinases in cell behaviour. Nat. Rev. Mol. Cell Biol. 4, 446–456.

Sahai, E., Ishizaki, T., Narumiya, S., Treisman, R., 1999. Transformation mediated by RhoA requires activity of ROCK kinases. Curr. Biol. 9, 136–145.

Sahai, E., Marshall, C.J., 2002. RHO-GTPases and cancer. Nat. Rev. Cancer 2, 133–142.

Salhia, B., Rutten, F., Nakada, M., Beaudry, C., Berens, M., Kwan, A., Rutka, J.T., 2005. Inhibition of Rho-kinase affects astrocytoma morphology, motility, and invasion through activation of Rac1. Cancer Res. 65, 8792–8800.

Shimokawa, H., Rashid, M., 2007. Development of Rho-kinase inhibitors for cardiovascular medicine. Trends Pharmacol. Sci. 28, 296–302.

Vecchiarelli-Federico, L.M., Cervi, D., Haeri, M., Li, Y., Nagy, A., Ben-David, Y., 2010. Vascular endothelial growth factor—a positive and negative regulator of tumor growth. Cancer Res. 70, 863–867.

Wozniak, M.A., Modzelewska, K., Kwong, L., Keely, P.J., 2004. Focal adhesion regulation of cell behavior. Biochim. Biophys. Acta 1692, 103–119.

THE JOURNAL OF BIOLOGICAL CHEMISTRY VOL. 286, NO. 29, pp. 26178–26187, July 22, 2011
© 2011 by The American Society for Biochemistry and Molecular Biology, Inc. Printed in the U.S.A.

Ultraviolet Irradiation Can Induce Evasion of Colon Cancer Cells from Stimulation of Epidermal Growth Factor*

Received for publication, March 16, 2011, and in revised form, June 5, 2011 Published, JBC Papers in Press, June 6, 2011, DOI 10.1074/jbc.M111.240630

Seiji Adachi[‡§1], Ichiro Yasuda[§], Masanori Nakashima[§], Takahiro Yamauchi[§], Junji Kawaguchi[§], Masahito Shimizu[§], Masahiko Itani[‡], Momoko Nakamura[‡], Yumi Nishii[‡], Takashi Yoshioka[¶], Yoshinobu Hirose[‖], Yukio Okano[¶], Hisataka Moriwaki[§], and Osamu Kozawa[‡]

From the Departments of [‡]Pharmacology, [§]Gastroenterology, and [¶]Molecular Pathobiochemistry, Gifu University Graduate School of Medicine, Gifu 501-1194, Japan and the [‖]Pathology Division, Gifu University Hospital, Gifu 501-1194, Japan

Receptor down-regulation is the most prominent regulatory system of EGF receptor (EGFR) signal attenuation and a critical target for therapy against colon cancer, which is highly dependent on the function of the EGFR. In this study, we investigated the effect of ultraviolet-C (UV-C) on down-regulation of EGFR in human colon cancer cells (SW480, HT29, and DLD-1). UV-C caused inhibition of cell survival and proliferation, concurrently inducing the decrease in cell surface EGFR and subsequently its degradation. UV-C, as well as EGFR kinase inhibitors, decreased the expression level of cyclin D1 and the phosphorylated level of retinoblastoma, indicating that EGFR down-regulation is correlated to cell cycle arrest. Although UV-C caused a marked phosphorylation of EGFR at Ser-1046/1047, UV-C also induced activation of p38 MAPK, a stress-inducible kinase believed to negatively regulate tumorigenesis, and the inhibition of p38 MAPK canceled EGFR phosphorylation at Ser-1046/1047, as well as subsequent internalization and degradation, suggesting that p38 MAPK mediates EGFR down-regulation by UV-C. In addition, phosphorylation of p38 MAPK induced by UV-C was mediated through transforming growth factor-β-activated kinase-1. Moreover, pretreatment of the cells with UV-C suppressed EGF-induced phosphorylation of EGFR at tyrosine residues in addition to cell survival signal, Akt. Together, these results suggest that UV-C irradiation induces the removal of EGFRs from the cell surface that can protect colon cancer cells from oncogenic stimulation of EGF, resulting in cell cycle arrest. Hence, UV-C might be applied for clinical strategy against human colon cancers.

Members of the EGF receptor (EGFR)[2] family, which are frequently overexpressed in several types of human cancers, including cancers of the lung (1), head and neck (2), prostate (3), breast (4), pancreas (5), and colon (6), have been associated with abnormal growth of these tumors. It is well known that exposure of cells to EGF results in rapid autophosphorylation of EGFR molecules at the cell surface (7–10), which upon activation lead to cell proliferation, motility, and enhanced survival (11). There are several mechanisms by which EGFR becomes oncogenic including: 1) increased EGFR expression levels, 2) autocrine and/or paracrine growth factor loops, 3) heterodimerization with other EGFR family members and cross-talk with heterologous receptor systems, 4) defective receptor down-regulation, and 5) activating mutations (12). In clinical trials, increasing evidence shows the efficacy of EGFR-targeted agents, including monoclonal antibodies on the one hand and tyrosine kinase inhibitors on the other (13).

Following activation, the ligand-receptor complexes are internalized and then enter endosomes, where the receptors and their ligands are sorted to various intracellular destinations (14). Thus, some receptors can be recycled back to the cell surface via early endosomes, and others are targeted to late endosomes and lysosomes for proteolytic degradation. There is increasing evidence that not only does receptor internalization act to terminate signaling, but that internalized endosome-associated receptors are also able to stimulate specific signal transduction pathways (15–17). Some agents that induce ligand-independent internalization and degradation of EGFR, such as the 225 mouse antibody (18) and gemcitabine (5), could have promising potential for cancer therapies. By contrast, it has previously been reported that the other factors or agents, such as oxidative stress (19) and cisplatin (20), can induce internalization of the EGFR but not degradation. They differ in their effects on the fate of the receptors, downstream signaling, and cell proliferation.

Receptor down-regulation is the most prominent regulatory system of EGFR signal attenuation and involves the internalization and subsequent degradation of the activated receptor in the lysosomes. With the current knowledge of the mechanism underlying EGFR down-regulation, this molecular event involves several important phosphorylation sites in EGFR. One is the phosphorylation at Tyr-1045, which provides a docking site for the ubiquitin ligase c-Cbl resulting in ubiquitination of the EGFR (10). The others are the phosphorylation at serine or threonine residues that is thought to represent a mechanism for attenuation of the receptor tyrosine kinase activity (21–23). Among the major sites of serine and threonine phosphorylation of the EGFR, it has previously been shown that the Ser-1046/7 phosphorylation site is required for EGFR desensitization in EGF-treated cells (23). Moreover, mutant EGFR at Ser-1046/7

* This work was supported in part by Grant-in-Aid for Scientific Research 22790639 (to S. A) from the Ministry of Education, Science, Sports and Culture of Japan and a grant by the Yokoyama Foundation for Clinical Pharmacology.

[1] To whom correspondence should be addressed: 1-1 Yanagido, Gifu 501-1194, Japan. Tel.: 81-58-230-6217; Fax: 81-58-230-6218; E-mail: seijiadachi0123@gmail.com.

[2] The abbreviations used are: EGFR, EGF receptor; UV-C, ultraviolet-C; MTT, 3-(4,5-dimethylthiazol-2-yl)-2,5-diphenyltetrazolium bromide; Rb, retinoblastoma protein; TAK-1, TGF-β-activated kinase-1; J, J/m^2; BrdU, bromodeoxyuridine; MKK, MAPK kinase; Ser-1046/7, Ser-1046/1047.

reportedly causes the inhibition of the EGF-induced endocytosis and down-regulation of cell surface receptors (22).

We have recently reported that phosphorylation of EGFR at serine 1046/7 via activation of p38 MAPK plays a pivotal role in down-regulation of EGFR induced by (−)-epigallocatechin gallate (24), anisomycin (25), and HSP90 inhibitor (26). Moreover, there is an evidence that cisplatin also induces EGFR internalization, which is mediated by p38 MAPK-dependent phosphorylation of the receptor at threonine 669 (20). Also, it has been shown that gemcitabine induces EGFR internalization and subsequent degradation, which may be a novel mechanism for gemcitabine-mediated cell death (5), whereas the activation of p38 MAPK is necessary for gemcitabine-induced cytotoxicity (27, 28). Taken together, serine phosphorylation of EGFR via p38 MAPK might be considered a new therapeutic target especially to counter cancer cells of the colon, lung, pancreas, and breast that highly express EGFR.

UV radiation from sunlight is sorted by wavelength regions: long wavelength UV-A (320–400 nm), medium wavelength UV-B (280–320 nm), and short wavelength UV-C (200–280 nm). In general, UV-A and UV-B are recognized the major carcinogenic components of sunlight (29). As for UV-C, it is used for studying DNA damage and cellular DNA repair process, although it does not actually exist in earth's surface because they are filtered out by the atmosphere. Although UV-C has been commonly applied for equipment such as water sterilization, recent studies show the possible application of UV-C against human cancer (30). However, its exact mechanism has not been fully clarified.

We have recently reported that the blockade of EGF stimulation significantly suppressed SW480 cell growth, suggesting that EGFR pathway plays an important role in proliferation of colon cancer cells (31). Therefore, we herein investigated the effect of UV-C on the down-regulation of EGFR in these cells and found that this induces the internalization and degradation of EGFR that indicates the removal of EGFR from cell membrane, and this action of UV-C can protect colon cancer cells from oncogenic stimulation such as EGF, resulting in cell cycle arrest.

EXPERIMENTAL PROCEDURES

Materials—SB203580, (5Z)-7-oxozeaenol, AG1478, and PD153035 were obtained from Calbiochem-Novabiochem Co. (La Jolla, CA). BIRB0796 was obtained from Dr. Philip Cohen (University of Dundee, Dundee, UK). Antibodies against total EGFR and GAPDH were obtained from Santa Cruz Biotechnology (Santa Cruz, CA). Antibodies against phospho-EGFR (Tyr-1045, Tyr-1068, and Ser-1046/7), phospho-p44/p42 MAPK, p44/p42 MAPK, phospho-p38 MAPK, p38 MAPK, phospho-SAPK/JNK, SAPK/JNK, phospho-TGF-β-activated kinase-1 (TAK-1), phospho-MKK3/6, cyclin D1, and phospho-retinoblastoma (Rb) were purchased from Cell Signaling (Beverly, MA). Antibodies against phospho-γH2A.X at Ser-139 (γH2AX) were purchased from Abcam (Cambridge, MA). An ECL Western blot detection system was purchased from GE Healthcare (Buckinghamshire, UK). Other materials and chemicals were obtained from commercial sources.

Cell Culture—SW480 and HT29, human colon cancer cells were grown in DMEM (Invitrogen) containing 10% FCS with penicillin (100 units/ml) and streptomycin (100 μg/ml) in a humidified 5% CO_2 incubator at 37 °C. DLD-1 cells, other human colon cancer cells, were grown in RPMI 1640 (Invitrogen). Two days after seeding, they were incubated in serum-free medium for 24 h as described previously (32).

Cell Proliferation Assay—The cells (3×10^3/well) were seeded onto 96-well plates, and 24 h later, the cells were exposed to the indicated doses (0–200 J/m^2 [J]) of UV-C after the aspiration of the growth medium. The cells were then incubated in DMEM with 1% FCS in a humidified 5% CO_2 incubator at 37 °C for 48 h. The remaining cells were finally counted by a 3-(4,5-dimethylthiazol-2-yl)-2,5-diphenyltetrazolium bromide (MTT) cell proliferation kit I (Roche Applied Science) in accordance with instructions of the manufacturer. BrdU incorporation was measured using cell Proliferation ELISA (Brd; Roche Applied Science). The cells (7×10^3/well) were seeded onto 96-well plates, and 48 h later, the cells were exposed to the indicated doses (0–50 J) of UV-C, just after the aspiration of the growth medium. The cells were then incubated in DMEM with 1% FCS for 24 h. They were then used for measurement according to the manufacturer's protocol. All of the assays were done in triplicate.

Clonogenic Survival Assay—The cells were grown in regular medium to 70% confluence and exposed to UV-C, AG1478, and PD153035 at the indicated doses. Twenty-four h after treatment, the cells were trypsinized and counted as usual. The cells (3×10^3) were reseeded into fresh tissue culture dishes and incubated for 7 days. Fresh media were added at day 4. At day 7, the media were removed, and the cells were fixed with 2 ml of clonogenic reagent (50% ethanol, 0.25% 1,9-dimethyl-methylene blue) for 45 min. They were then washed with PBS twice, and the blue colonies were counted.

UV-C Exposure—UV-C exposure of cells was performed in a UV-C 500 UV Crosslinker (GE Healthcare) by which we used 10–200 J/m^2 (J) of UV at 254 nm. After aspiration of the growth media, the cells were exposed to the indicated doses of UV-C in 20 s and then incubated for the indicated times.

Western Blot Analysis—The cells were lysed in lysis buffer (20 mM Tris, pH 7.5, 150 mM NaCl, 1 mM EDTA, 1 mM EGTA, 1% Triton X-100, 2.5 mM sodium pyrophosphate, 50 mM NaF, 50 mM HEPES, 1 mM Na_3VO_4, and 2 mM PMSF) and scraped from the Petri dishes. Protein extracts were examined by Western blot analysis as previously described (33). The protein was fractionated and transferred onto an Immune-Blot PVDF membrane (Bio-Rad). The membranes were blocked with 5% fat-free dry milk in PBS containing 0.1% Tween 20 for 30 min before incubation with the indicated primary antibodies. Peroxidase-labeled antibodies raised in goat against rabbit IgG were used as second antibodies. Peroxidase activity on the membrane was visualized on x-ray film by means of the ECL Western blot detection system.

Immunofluorescence Microscopy Studies—Immunofluorescence microscopy studies were performed as described previously (25). The cells grown on coverslip-bottomed dishes were first treated with either SB203580 or siRNA-p38 MAPK, followed by exposure to anti-EGFR antibodies for 15 min in RPMI

containing 1% BSA. They were then exposed to UV-C (30 J) and incubated in DMEM without FCS for additional 30 min. They were then fixed with 4% paraformaldehyde for 10 min on ice and then exposed to 0.1% Triton X-100 for 10 min to permeabilize the cell membrane. They were followed by exposure to Alexa Fluor 546®-conjugated donkey anti-mouse IgG antibodies (Invitrogen) and DAPI (Wako, Tokyo, Japan) for 1 h. The cells were then examined by fluorescence microscopy, BIOREVO (BZ-9000) (Keyence, Tokyo, Japan) according to the manufacturer's protocol.

siRNA Protocol—Predesigned siRNAs targeting p38 MAPK (On-TARGET plus Duplex J-003512–20, human MAPK14) was purchased from Thermo Fisher Scientific K.K. (Yokohama, Japan). Sequences are as follows: sense, GGAAUUCAAUGAUGUGUAUUU and antisense, AUACACAUCAUUGAAUUCCUU. Transfection was performed according to the manufacturer's protocol (Bio-Rad). In brief, 5 μl of siLentFect (Bio-Rad) and finally 100 nM of siRNA were diluted with Opti-MEM, preincubated at room temperature for 20 min, and then added to the culture medium containing 10% FCS. The cells were incubated at 37 °C for 48 h with siRNA-siLentFect complexes and subsequently harvested for preparation of Western blot analysis.

Quantification of Cell Surface EGFR by ELISA—Quantification of cell surface EGFR was performed as described previously (32). In brief, SW480 cells were pretreated with the indicated compounds and then exposed to the mouse anti-EGFR antibody (Santa Cruz Biotechnology) that recognizes the extracellular domain of the EGFR (1:50 dilution) in DMEM containing 1% BSA for 15 min at 37 °C. The cells were then incubated for the indicated times after exposure to UV-C (30 J) and then fixed with 4% paraformaldehyde for 10 min on ice. After blocking with 1% BSA in PBS for 1 h, the cells were exposed to an anti-mouse IgG, horseradish peroxidase-linked whole antibody (GE Healthcare) for 1 h at room temperature, followed by washing four times with PBS containing 1% BSA. Finally, the cells were exposed to 50 μl of 1-Step™ Ultra TMB-ELISA reagent (Pierce) for 5 min at room temperature. Fifty μl of 2 M sulfuric acid was then added to each well to stop the reaction. The absorbance of each sample at 450 nm was then measured.

Densitometric Analysis—The densitometric analysis was performed using scanner and image analysis software (Image J version 1.32). The background-subtracted signal intensity of each protein signal was normalized by the respective control signal. All of the data were obtained from at least three independent experiments.

Detection of UV-C-caused DNA Damage—DNA damage caused by UV-C was examined by detection of phospho-H2A.X at Ser-139 (γH2AX). The cells were pretreated with or without 1 μM of BIRB0790 for 1 h and then exposed to UV-C (30 J), followed by incubation for the indicated periods. They were then lysed in radioimmune precipitation assay buffer (50 mM Tris-HCl, pH 7.4, 1% Nonidet P-40, 0.25% sodium deoxycholate, 150 mM NaCl, 1 mM EGTA, 1 mM NaF, 1 mM Na_3VO_4, and complete protease inhibitor mixture tablets (Hoffmann-La Roche Inc. Nutley, NJ)). After sonication for 10 s, the protein extracts were quantified and examined by Western blot analysis. As for immunofluorescence study, the cells grown on coverslip-bottomed dishes were first treated with or without 1 μM of BIRB0790. They were then exposed to UV-C (30 J) and incubated for 3 h, followed by fixation, permeabilization, and exposure to anti-γH2AX for 1 h. They were then exposed to Alexa Fluor 546®-conjugated donkey anti-rabbit IgG antibodies and DAPI for 1 h. Finally, the cells were examined by fluorescence microscopy.

Statistical Analysis—The data were analyzed by analysis of variance followed by the Bonferroni method for multiple comparisons between the indicated pairs, and a $p < 0.05$ was considered significant.

RESULTS

UV-C and EGFR Kinase Inhibitors Inhibited Colon Cancer Cell Proliferation—We first investigated the effect of UV-C on the proliferation of SW480 cells using MTT. As shown in Fig. 1*A*, the IC_{50} value of UV-C in SW480 cells was ~80 J. Also, the Brd incorporation assay revealed that SW480 cell proliferation was significantly suppressed when the cells were treated with the increasing dose of UV-C (Fig. 1*B*, black bars). We also observed similar effects of UV-C in HT29 and DLD-1 cells, other colon cancer cells (Fig. 1*B*, *gray* and *white bars*). Therefore, it is likely that UV-C has suppressive effects on colon cancer cell proliferations. We have recently reported that anti-EGFR neutralizing antibodies significantly suppressed cell growth in SW480 colon cancer cells (31). In this study, we used two kinds of EGFR kinase inhibitor, AG1478 and PD153035, and examined the inhibitory effect of EGFR kinase activity on colon cancer cell proliferation. MTT assay shows that these inhibitors suppressed cell proliferation (Fig. 1*C*). In addition, Fig. 1*D* revealed the suppressive effects of UV-C as well as EGFR kinase inhibitors on colony formations, indicating the reduction of capability of SW480 cells to survive and replicate (34).

The ternary complex of cyclin D/cyclin-dependent kinase 4 and p27 Kip1 requires extracellular mitogenic stimuli for the release and degradation of p27 concomitant with a rise in cyclin D levels to affect progression through the restriction point and phospho-Rb-dependent entry into the S phase (35), indicating that increasing levels of cyclin D1 and phospho-Rb promote cell cycle, resulting in cell proliferation. Because EGFR kinase inhibitors also suppressed the phosphorylation of Rb as well as the protein level of cyclin D1 (Fig. 1*E*), it is likely that EGFR signaling plays a critical role in proliferation of colon cancer cells.

UV-C Induced Down-regulation of EGFR and Cell Cycle Arrest in Colon Cancer Cells—Overexpressed EGFR plays an oncogenic role in colon cancer cells, and its down-regulation is the most prominent regulatory system of EGFR signal attenuation (36). Whereas it has previously been reported that UV induces internalization and endosome arrest of EGFR in HeLa epidermal carcinoma cells (30, 37), we investigated the effect of UV-C on EGFR signaling pathway in SW480 cells. In Fig. 2*A*, UV-C caused a marked decrease in the amount of cell surface EGFRs within 10–30 min, whereas they were not affected in unstimulated SW480 cells. Moreover, UV-C markedly decreased the protein level of EGFR in SW480, HT29, and DLD-1 cells (Fig. 2*B*), thus suggesting that UV-C induces EGFR

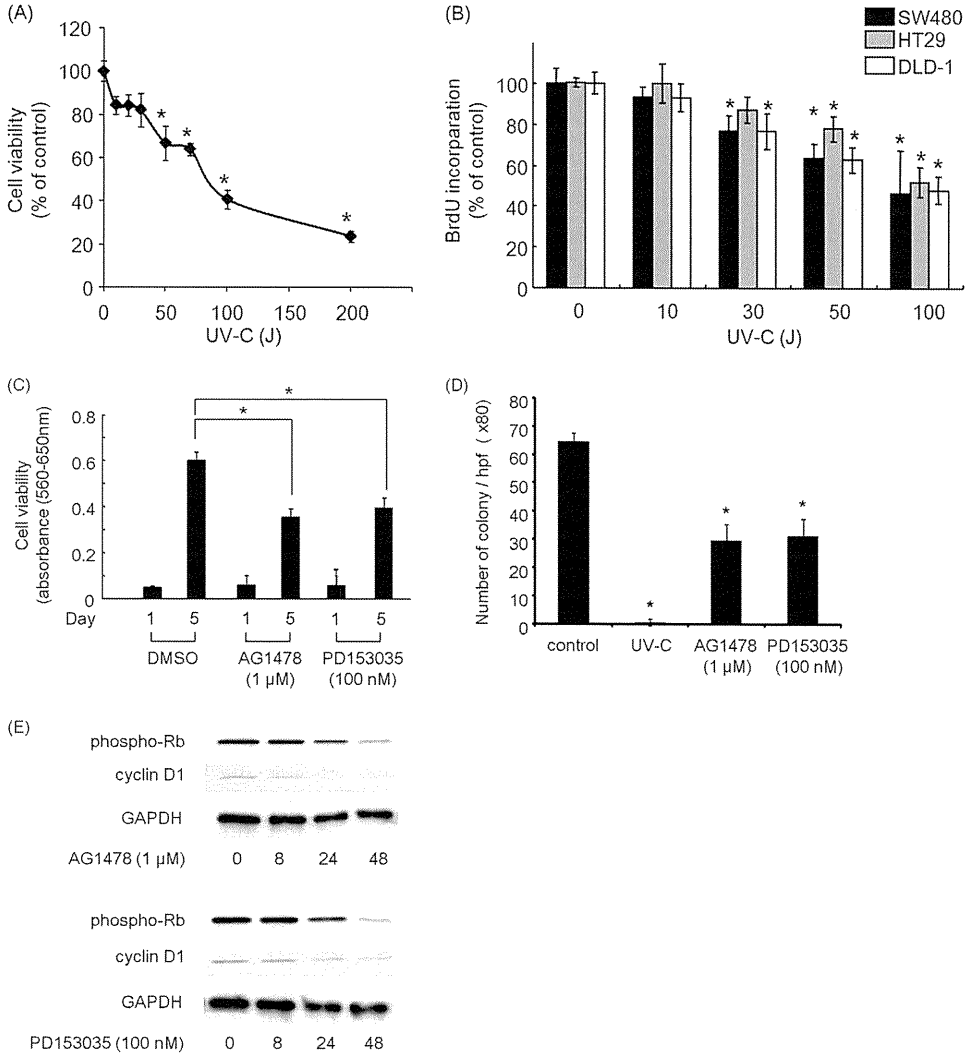

FIGURE 1. **UV-C and EGFR kinase inhibitors inhibited cell survival and proliferation in colon cancer cells.** *A*, SW480 cells were exposed to UV-C for 48 h under medium containing 3% FCS, and then the remaining cells were counted by MTT cell proliferation kit I. The results are expressed as percentages of growth, with 100% representing untreated control cells. *B*, the indicated cells (SW480, HT29, and DLD-1) were exposed to UV-C for 24 h under medium containing 3% FCS, and the measurement of BrdUrd incorporation during DNA synthesis was performed using cell proliferation ELISA (Brd). The results are expressed as percentage of incorporation, with 100% representing control cells. *C*, SW480 cells were treated with 1 μM of AG1478, 100 nM of PD153035, or vehicle for 4 days under medium containing 3% FCS, and then the remaining cells were counted by the MTT cell proliferation kit I. *D*, the attached SW480 cells were exposed to 30 J of UV-C, 1 μM of AG1478, or 100 nM of PD153035 and incubated for 24 h. After trypsinization, the counted cells (3×10^3) were reseeded into new culture dishes and incubated for 7 days. The cells were then fixed with clonogenic reagent (see "Experimental Procedures"), and the average numbers of colonies from five randomly chosen fields (×80) were counted, respectively. *E*, SW480 cells were treated with 1 μM of AG1478 or 100 nM of PD153035 for the indicated periods. Protein extracts were then harvested and examined by Western blotting using antibodies against phospho-specific Rb, cyclin D1, and GAPDH. All of the assays were done in triplicate. The *error bars* designate S.D. of triplicate assays. The *asterisks* indicate a significant difference ($p < 0.05$), compared with the control.

down-regulation in colon cancer cells. Moreover, UV-C (30 J) time-dependently decreased the protein level of cyclin D1 in addition to phospho-Rb (Fig. 2*C*). Also, increasing dose of UV-C caused the decrease in both of cyclin D1 expression level and phospho-Rb, concurrently with the decrease in EGFR protein level (Fig. 2*D*). Therefore, it is probable that UV-C-induced EGFR down-regulation is correlated to cell cycle arrest in colon cancer cells.

UV-C Induced Phosphorylation of EGFR at Ser-1046/7, not Tyrosine Residues in Colon Cancer Cells—To elucidate how UV-C causes EGFR down-regulation in colon cancer cells, we examined the effects of UV-C on the phosphorylation of EGFR at several residues. Although UV-C had slight, but no appreciable effect on phosphorylation of EGFR at Tyr-1045 and Tyr-1068, both of which are known as autophosphorylation sites (8–10), UV-C markedly induced phosphorylation of EGFR at Ser-1046/7 in SW480 cells (Fig. 3). This phosphorylation at Ser-1046/7 appeared at 10 min after exposure to UV-C (30 J) and reached maximum at 60 min and decreased thereafter (Fig. 3*A*). In addition, this appeared when the cells were exposed to UV-C at a dose over 20 J (Fig. 3*B*).

p38 MAPK Was Involved in the Phosphorylation of EGFR at Ser-1046/7, and Subsequently Its Internalization Was Induced by UV-C in Colon Cancer Cells—To clarify how UV-C induces EGFR phosphorylation at serine residues, we next examined the effect of UV-C on the activations of MAPK cascades. UV-C induced phosphorylation of p44/p42 MAPK, SAPK/JNK, and p38 MAPK within 10–20 min in SW480 cells (Fig. 4*A*). These

results led us to further investigate which protein kinase plays a critical role in the phosphorylation of EGFR at serine residues induced by UV-C in colon cancer cells.

Although we showed that UV-C caused a rapid decrease in the amount of cell surface EGFR (Fig. 2*A*), we next examined whether UV-C also induces changes in the cellular localization of the EGFR in SW480 cells using fluorescence microscopy. As shown in Fig. 4*B*, EGFR was mainly localized on the cell surface (Fig. 4*B*, *panel 1*). As expected, UV-C caused the internalization of EGFR (Fig. 4*B*, *panel 2*), and moreover, when the cells were pretreated with SB203580, a p38 MAPK-selective inhibitor (38), the internalization of EGFR was virtually inhibited (Fig. 4*B*, *panel 4*). We also obtained similar results using siRNA-p38 MAPK (Fig. 4*C*). These results strongly suggest that activation of p38 MAPK truly mediates the UV-C effect on the cellular localization of EGFR in colon cancer cells.

As depicted in Fig. 4*D*, BIRB0790, another p38 MAPK-selective inhibitor (39) in addition to SB203580 significantly suppressed the phosphorylation of EGFR at Ser-1046/7 induced by UV-C (Fig. 4*D*), although that was not suppressed when the cells were pretreated with PD98059 (40) and SP600125 (41), which can inhibit the activation of MEK1/2 and SAPK/JNK, respectively (data not shown). To verify our results shown in Fig. 4*D*, we further performed siRNA experiment and observed that UV-C-caused phosphorylation of EGFR at Ser-1046/7 was clearly suppressed by siRNA-p38 MAPK, whereas negative control siRNA did not have any effects (Fig. 4*E*). We also verified that these findings were applicable in HT29 and DLD-1 cells (Fig. 4*F*). Together, we strongly suggest that phosphorylation of EGFR at Ser-1046/7 induced by UV-C was also mediated through the p38 MAPK pathway in colon cancer cells.

Phosphorylation of p38 MAPK Induced by UV-C Was Mediated through TAK-1 in Colon Cancer Cells—TAK-1 is activated by TGFβ as well as cytokines, including interleukin-1 (42, 43). TAK-1 is also known to be a kinase of MAPK kinase (MKK) 3/6 (44–46). Moreover, MKK3 can phosphorylate p38 MAPK (47). Therefore, we examined the effect of UV-C on TAK-1 to examine the upstream signaling for activation of p38 MAPK. Of interest, UV-C induced phosphorylation of TAK-1 as well as MKK3/6 (Fig. 5*A*). Moreover, the inhibition of TAK-1 using (5Z)-7-oxozeaenol restored UV-C-induced phosphorylation of EGFR (Ser-1046/7), MKK3/6, and p38 MAPK (Fig. 5*B*). Therefore, it is most likely that UV-C induces activation of p38 MAPK via TAK-1.

Degradation of EGFR and Cyclin D1 Induced by UV-C Was Blocked by the Inhibition of p38 MAPK in Colon Cancer Cells—We next investigated the involvement of p38 MAPK in UV-C-induced degradation of EGFR and cyclin D1. As depicted in Fig. 6*A*, the protein level of both EGFR and cyclin D1 were decreased when the cells were treated with UV-C (Fig. 6*A*, *lane 2* compared with *lane 1*), consistently with the above results shown in Fig. 2 (*B–D*). As expected, pretreatment of the cells with SB203580 significantly inhibited UV-C-induced degradation of cyclin D1 as well as EGFR (Fig. 6*A*, *lane 4* compared with *lane 3*). Similarly, the protein level of both EGFR and cyclin D1 were not decreased by UV-C in the cells that were transfected with p38 MAPK-siRNA (Fig. 6*B*, *lane 4* compared with *lane 3*), in comparison with the cells transfected with negative control (Fig. 6*B*, *lane 2* compared with *lane 1*). These results strongly suggest that activation of p38 MAPK plays a critical role in the down-regulation of EGFR induced by UV-C in colon cancer cells.

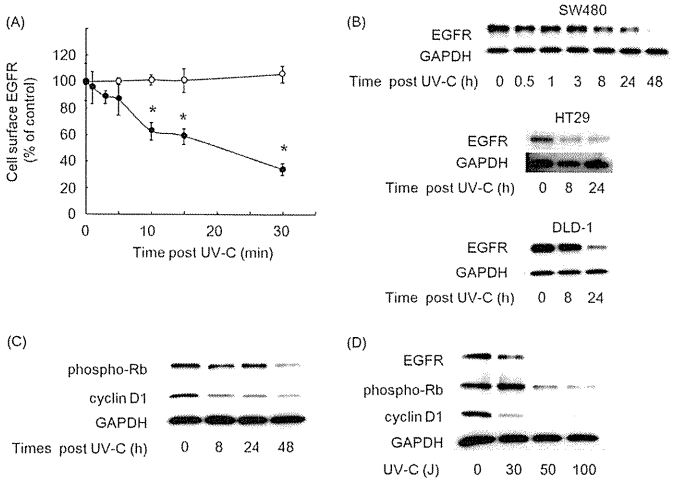

FIGURE 2. **UV-C caused down-regulation of the EGFR and cell cycle arrest in colon cancer cells.** *A*, UV-C induced the decrease in the cell surface amount of EGFR in SW480 cells. The *line graph* shows the quantification data for the cell surface amount of EGFR analyzed by ELISA (see under "Experimental Procedures"). ○, unstimulated SW480 cells; ●, SW480 cells exposed to 30 J of UV-C. *B*, the indicated cells (SW480, HT29, and DLD-1) were exposed to UV-C at a dose of 30 J and then incubated for the indicated periods. *C*, SW480 cells were exposed to 30 J of UV-C for the indicated periods. *D*, SW480 cells were exposed to UV-C at the indicated doses and then incubated for 24 h. Protein extracts were then harvested and examined by Western blotting using antibodies against EGFR, phospho-specific Rb, cyclin D1, and GAPDH. Representative results from triplicate independent experiments with similar results are shown.

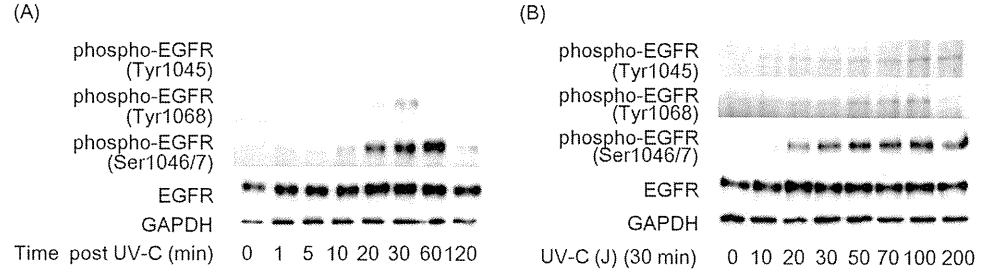

FIGURE 3. **Effect of UV-C on the phosphorylation of EGFR at Ser-1046/7 in colon cancer cells.** *A*, SW480 cells were exposed to UV-C at a dose of 30 J for the indicated periods. *B*, SW480 cells were exposed to UV-C at the indicated doses and then incubated for 1 h. Protein extracts were then harvested and examined by Western blotting using anti-phospho-EGFR at Tyr-1045, Tyr-1068, and Ser-1046/7, anti-EGFR, and anti-GAPDH antibodies. Representative results from triplicate independent experiments with similar results are shown.

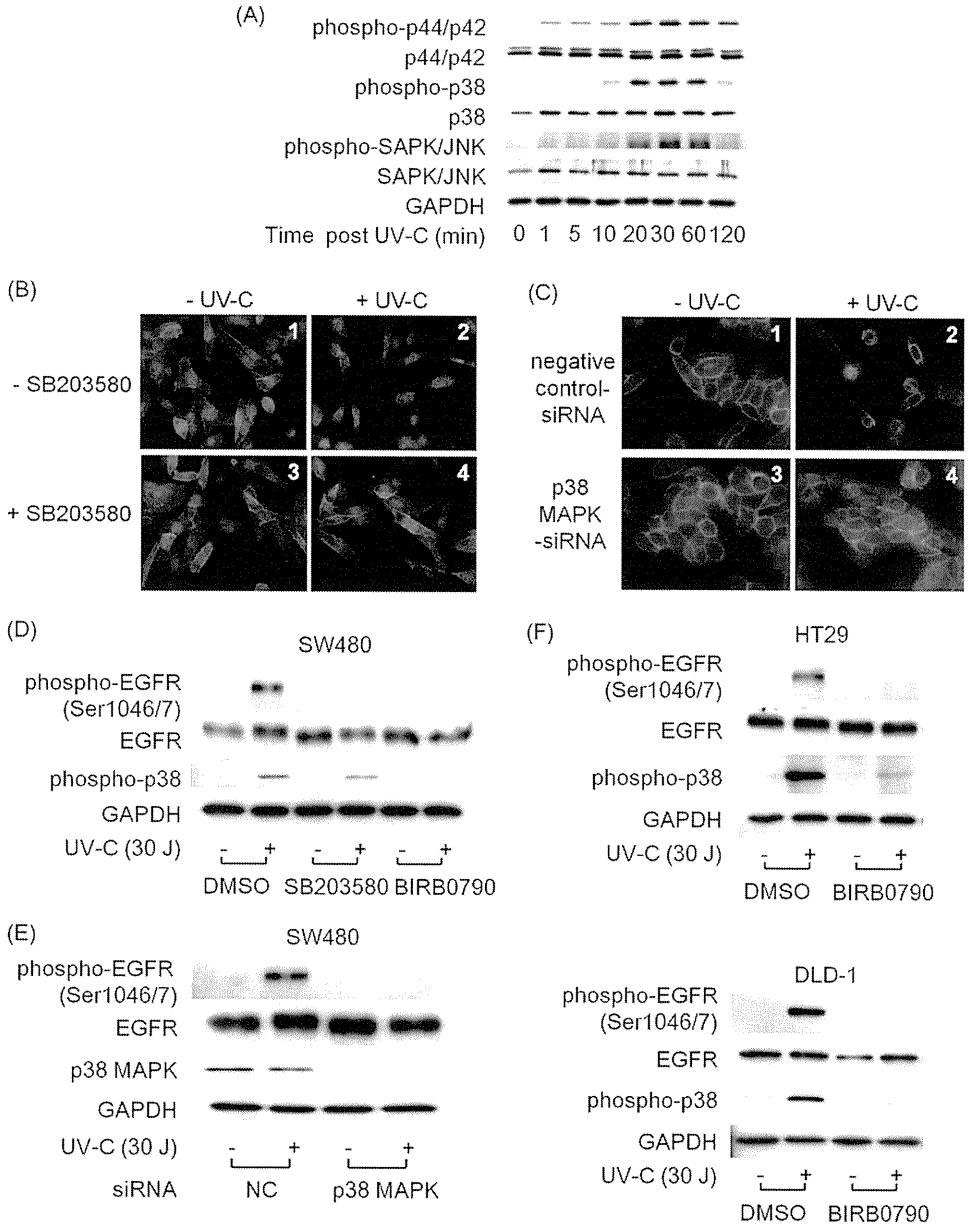

FIGURE 4. **Effects of p38 MAPK on the internalization and phosphorylation of EGFR at Ser-1046/7 in colon cancer cells.** *A*, SW480 cells were exposed to UV-C at 30 J and then incubated for the indicated periods. Protein extracts were then harvested and examined by Western blotting using anti-phospho-p44/p42 MAPK, anti-p44/p42 MAPK, anti-phospho-p38 MAPK, anti-p38 MAPK, anti-phospho-SAPK/JNK, anti-SAPK/JNK, and anti-GAPDH antibodies. *B*, SW480 cells were pretreated with or without 10 μM of SB203580 for 1 h and then labeled for 15 min at 37 °C with anti-EGFR antibodies that recognize the extracellular domain of the EGFR. *C*, SW480 cells were incubated with 100 nM of p38 MAPK-siRNA or negative control siRNA at 37 °C for 48 h in FCS-free opti-MEM and then labeled for 15 min at 37 °C with anti-EGFR antibodies. They were then exposed to UV-C (30 J) and incubated for additional 1 h, followed by fixation with paraformaldehyde. After permeabilization of the cells with 0.1% Triton X-100, the cells were treated with Alexa 546-conjugated anti-mouse secondary antibody for EGFR (*red signal*) and DAPI (*blue signal*) for 1 h and then examined by fluorescence microscope. *D*, SW480 cells were pretreated with 10 μM of SB203580 or 1 μM of BIRB0790 for 1 h and then exposed to UV-C at 30 J and then incubated for additional 1 h. *E*, SW480 cells were incubated with 100 nM of p38 MAPK-siRNA or negative control siRNA at 37 °C for 48 h in FCS-free opti-MEM, followed by exposure to UV-C (30 J) for 1 h. *F*, HT29 and DLD-1 cells were pretreated with 1 μM of BIRB0790 for 1 h and then exposed to UV-C at 30 J and then incubated for additional 1 h. Protein extracts were then prepared and examined by Western blotting using antibodies against phospho-EGFR at Ser-1046/7, EGFR, phospho-p38 MAPK, and p38 MAPK, respectively. An antibody to GAPDH was used to control for protein loading. Representative results from triplicate independent experiments with similar results are shown.

Pretreatment with UV-C Can Protect Colon Cancer Cells from EGF Stimulation—It is well known that exposure of cells to EGF stimulation results in rapid autophosphorylation of EGFR molecules at the cell surface (7–10), which upon activation lead to cell proliferation, motility, and enhanced survival (11). Moreover, through EGF binding to cell surface EGFR, it activates an extensive network of signal transduction pathways including Akt pathways, which regulates multiple biological processes including survival, proliferation, and cell growth (48, 49). We next investigated the effect of pretreatment with UV-C on EGF-induced phosphorylation of EGFR and Akt in SW480 cells. When the cells were not exposed to UV-C or EGF, EGFR at any residue and Akt were not phosphorylated (Fig. 7*A*, *lane 1*). Indeed, UV-C caused phosphorylation of EGFR at Ser-1046/7 (Fig. 7*A*, *second panel*), consistently with the above results shown in Fig. 3. Interestingly, although stimulation with

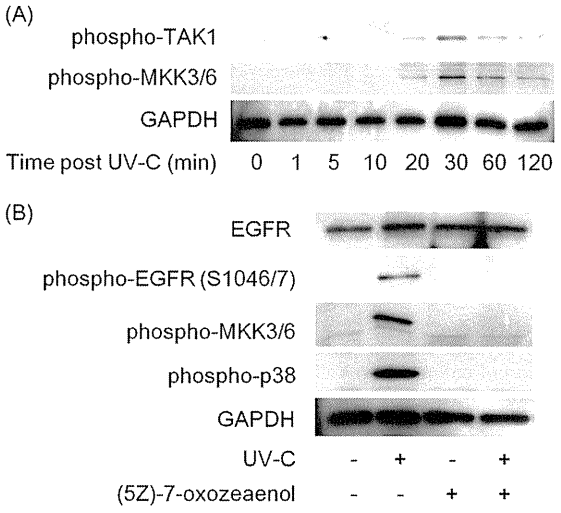

FIGURE 5. **The involvement of TAK-1 in UV-C-induced activation of p38 MAPK in colon cancer cells.** *A*, SW480 cells were exposed to UV-C at 30 J and then incubated for the indicated periods. *B*, SW480 cells were pretreated with or without the 300 nM of (5Z)-7-oxozeaenol, as a TAK-1 inhibitor, for 2 h and then exposed to UV-C (30 J) and incubated for additional 30 min. Protein extracts were then harvested and examined by Western blotting using anti-EGFR, phospho-EGFR (Ser-1046/7), phospho-TAK1, anti-MKK3/6, anti-p38 MAPK, and anti-GAPDH antibodies. Representative results from triplicate independent experiments with similar results are shown.

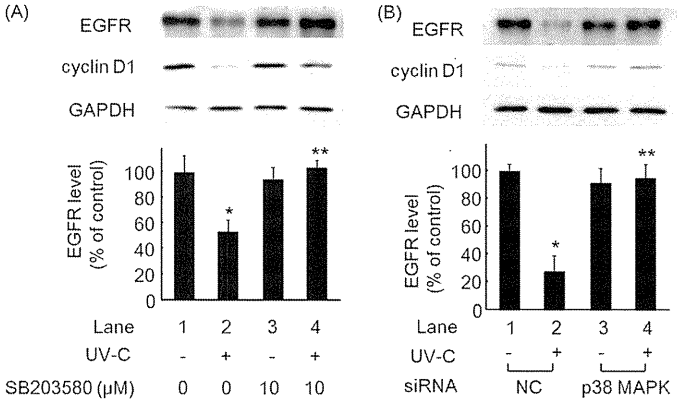

FIGURE 6. **The inhibition of p38 MAPK restored UV-C-induced degradation of the EGFR in colon cancer cells.** *A*, SW480 cells were pretreated with or without 10 μM of SB203580 for 1 h and then exposed to UV-C at 30 J, followed by incubation for 8 h. *B*, SW480 cells were incubated with 100 nM of p38 MAPK-siRNA or negative control (*NC*) siRNA at 37 °C for 48 h in FCS-free opti-MEM, followed by exposure to UV-C (30 J). Protein extracts were then prepared and examined by Western blotting using anti-EGFR and anti-cyclin D1 antibodies, respectively. An antibody to GAPDH was used to control for protein loading. The *bar graph* shows quantification data for the relative levels of EGFR, after normalization with respect to GAPDH, as determined by densitometry. The *asterisks* indicate significant increase (*, $p < 0.05$ compared with *lane 1*; **, $p < 0.05$ compared with *lane 2*). Representative results from triplicate independent experiments with similar results are shown.

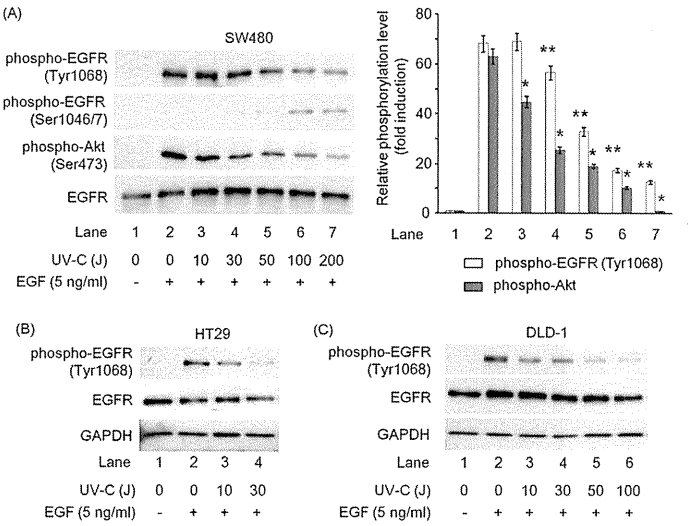

FIGURE 7. **Effects of exposure to UV-C before EGF stimulation on the phosphorylation of EGFR in colon cancer cells.** *A*, SW480 cells were pretreated with UV-C at the indicated doses of UV-C for 1 h and then exposed to 5 ng/ml of EGF for another 5 min. Protein extracts were then harvested and examined by Western blotting using anti-phospho-EGFR at Tyr-1068 and Ser-1046/7, anti-phospho-Akt, and anti-EGFR antibodies. The *bar graph* shows quantification data for the relative phosphorylation levels of EGFR and Akt, after normalization with respect to EGFR, as determined by densitometry. *, $p < 0.05$ compared with the control (EGF-induced phosphorylation of EGFR at Tyr-1068 in *lane 2*); **, $p < 0.05$ compared with the control (EGF-induced phosphorylation of Akt in *lane 2*). *B* and *C*, HT29 (*B*) and DLD-1 (*C*) cells were pretreated with UV-C at the indicated doses of UV-C for 1 h and then exposed to 5 ng/ml of EGF for another 5 min. Protein extracts were then harvested and examined by Western blotting using anti-phospho-EGFR at Tyr-1068, anti-EGFR, and anti-GAPDH antibodies. Representative results from triplicate independent experiments with similar results are shown.

EGF caused the phosphorylation of EGFR at tyrosine residues and Akt (Fig. 7*A*, *first* and *third panels*, *lane 2*), these phosphorylations were significantly suppressed when the cells were exposed to the increasing doses of UV-C before EGF stimulation (Fig. 7*A*, *first* and *third panels*). In cases of HT29 and DLD-1 cells, UV-C also had the suppressive effects on EGF-induced activation of EGFR (Fig. 7, *B* and *C*). These results strongly suggest that UV-C caused the evasion of colon cancer cells from EGF stimulation because UV-C can remove EGFR from cell membrane.

DNA Damage Is Not Involved in UV-C-induced EGFR Down-regulation in Colon Cancer Cells—DNA damage, provoked by UV radiation, evokes a cellular damage response composed of activation of stress signaling and DNA checkpoint functions (29). In addition, DNA double-strand breaks introduced into mammalian cells result in the specific phosphorylation of histone H2A.X at Ser-139, named γH2AX (50). We examined whether DNA damage correlates to UV-C-induced EGFR down-regulation via p38 MAPK. Although BIRB0790 clearly inhibited phosphorylation of p38 MAPK (Fig. 8*B*), immunofluorescence study and Western blotting showed that it had little effect on UV-C-induced γH2AX (Fig. 8, *A* and *B*). Therefore, it seems unlikely that DNA damage is involved in UV-C-induced EGFR down-regulation via p38 MAPK.

DISCUSSION

Whereas UV irradiation reportedly has many effects on skin, including inflammation, immunosuppression, and alterations in the extracellular matrix, in addition to accelerated skin aging (51), in the present study we demonstrated that UV-C has a potent anti-cancer effect by decreasing EGFR protein level in colon cancer cells. First, we showed that UV-C caused anti-survival and proliferative effects on SW480, HT29, and DLD-1 cells (Fig. 1). Because EGFR activation has been shown to be oncogenic (9), and we here showed that colon cancer cell proliferation depended on EGFR signaling (Fig. 1, *C–E*), we examined the effect of UV-C on the EGFR signaling and found that UV-C induced internalization and subsequent down-regula-

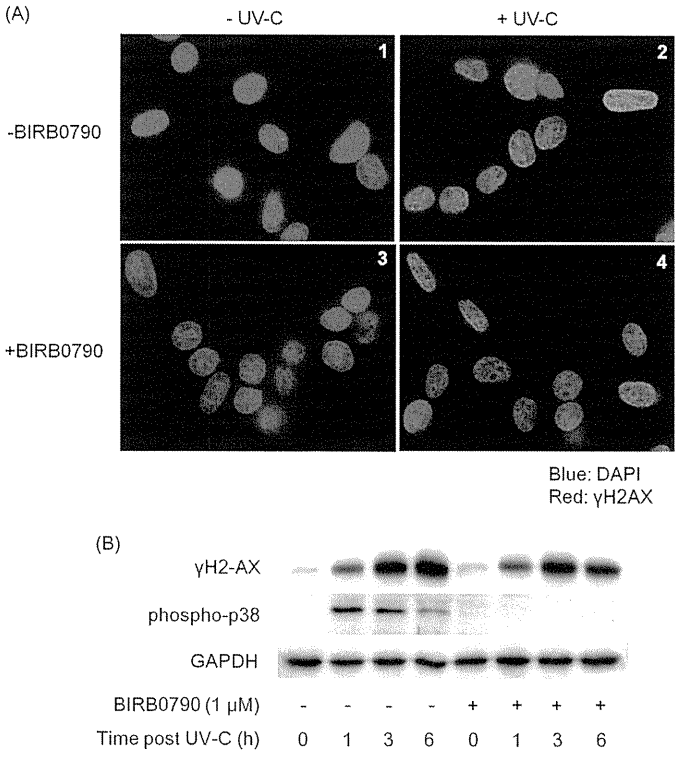

FIGURE 8. **The involvement of DNA damage in UV-C-induced activation of p38 MAPK in colon cancer cells.** *A*, SW480 cells grown on coverslip-bottomed dishes were pretreated with or without 1 μM of BIRB0790 and then exposed to UV-C (30 J) and incubated for another 3 h, and the cells were examined by fluorescence microscopy. *Red signals*, γH2AX; *blue signals*, DAPI. *B*, SW480 cells were pretreated with or without 1 μM of BIRB0790 for 1 h and then exposed to 30 J of UV-C, followed by incubation for another 3 h. Protein extracts were then harvested and examined by Western blotting using anti-γH2AX, anti-phospho-p38 MAPK, and anti-GAPDH antibodies. Representative results from triplicate independent experiments with similar results are shown.

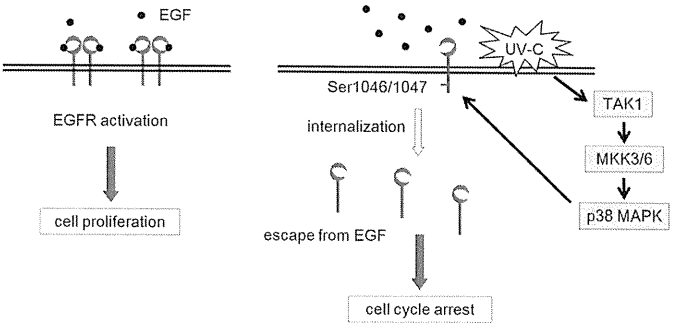

FIGURE 9. **Schematic representation of the effect of UV-C on EGF-induced proliferation of colon cancer cells.** After EGF binds to cell surface EGFR, it undergoes dimerization and autophosphorylation at tyrosine residues, and this triggers EGFR-related downstream signaling, leading to cell proliferation (7–10). By contrast, UV-C causes serial phosphorylation of TAK1, MKK3/6, and p38 MAPK and subsequent phosphorylation of EGFR at Ser-1046/7 but not tyrosine residues, and the serine-phosphorylated EGFR are internalized and eventually degraded. Therefore, UV-C can escape colon cancer cells from oncogenic stimulation of EGF, because EGF hardly binds to the internalized EGFR caused by UV-C.

tion of the EGFR and also decreased the protein level of cyclin D1 and phospho-Rb (Fig. 2), suggesting that the anti-cancer effect of UV-C could be due to cell cycle arrest in colon cancer cells.

In addition, we showed in Fig. 3 that UV-C caused a marked phosphorylation of EGFR at Ser-1046/7; however, UV-C failed to induce phosphorylation at Tyr-1045, the major c-Cbl binding site, as well as Tyr-1068, the Grb2 adaptor protein-binding site (8), in contrast to the prominent phosphorylation induced by EGF as we have previously shown (25). Moreover, although UV-C caused activation of p44/p42 MAPK, p38 MAPK, or SAPK/JNK (Fig. 4*A*), we observed that the inhibition of p38 MAPK suppressed EGFR internalization (Fig. 4, *B* and *C*). In addition, p38 MAPK was involved in phosphorylation at Ser-1046/7 (Fig. 4, *D–F*) and subsequent degradation (Fig. 6) of the EGFR induced by UV-C. Moreover, UV-C-induced activation of p38 MAPK was mediated through TAK-1 (Fig. 5). We also examined the effect of UV-C on apoptosis signal-regulating kinase 1, a MAPK kinase kinase, because apoptosis signal-regulating kinase 1 is activated in response to a variety of stress-related stimuli and activates MKK3, which in turn activate p38 MAPK (52). However, UV-C had no appreciable effect on phosphorylation of apoptosis signal-regulating kinase 1 at Ser-967 and Thr-845 (data not shown). Furthermore, we found in colon cancer cells that pretreatment with UV-C before EGF stimulation significantly suppressed the phosphorylation of EGFR at tyrosine residues and Akt (Fig. 7), indicating that UV-C can evade cells from oncogenic stimulation of EGF. In addition, as shown in Fig. 8, it seems unlikely that DNA damage is involved in UV-C-induced EGFR down-regulation via p38 MAPK. However, our present findings do not evaluate and cannot completely eliminate the possibility that DNA damage plays a role in UV-C-induced cell cycle arrest.

Whereas we have recently reported that the blockade of EGF stimulation significantly suppressed cell growth (31), we herein demonstrated that proliferation of colon cancer cells depended on the EGFR kinase activity, thus suggesting that the desensitization of EGFR signaling is a promising target against human colon cancer. In addition, an early work showed that exposure to UV light induced clustering and internalization of cell surface EGFR, and inhibition of clustering or receptor down-regulation attenuates UV responses (53), which is consistent with our present findings that internalization and subsequent degradation of EGFR induced by UV-C leads to cell cycle arrest of colon cancer cells by causing its phosphorylation at serine residues via p38 MAPK. Because it is generally understood that tyrosine phosphorylation results in cancer cell proliferation (9), these results also suggest the potential availability of UV-C for human colon cancer therapy because UV-C can cause EGFR down-regulation without oncogenic activation (Fig. 3). Moreover, Zwang and Yarden (30) previously reported that abrogating EGFR internalization reduces the efficacy of chemotherapy-induced cell death and EGFR internalization enhances the cytotoxic effect of cisplatin by preventing EGFR-mediated survival signaling, which may underlie interactions between chemotherapy and EGFR-targeting drugs. Therefore, our findings also provide the possibility of a new combination of conventional chemotherapy and UV-C for human colon cancer.

Our present study combined with previous findings is summarized in Fig. 9 as follows; when the cells are exposed to EGF stimulation, EGFR undergoes dimerization and tyrosine phosphorylation that directs the cells into cell proliferation (9). Subsequently, c-Cbl, a ubiquitin ligase, can bind to EGFR and cause ubiquitination and degradation of the EGFR (10, 54). By con-

trast, UV-C has little effect on EGFR phosphorylation at tyrosine residues, indicating that adequate dose of UV-C fails to exert the cell growth signals. However, UV-C induced serial phosphorylation of TAK1, MKK3/6, and p38 MAPK and subsequent phosphorylation of EGFR at Ser-1046/7. With time, EGFR molecules are internalized and eventually degraded. Therefore, pretreatment of the cells with UV-C can protect colon cancer cells from oncogenic stimulation such as EGF.

We have previously reported that (−)-epigallocatechin gallate, as well as HSP90 inhibitors, causes down-regulation of the EGFR via phosphorylation at Ser-1046/7 through p38 MAPK in human cancer cells (24, 26). Additionally, accumulating evidence shows that activation of p38 MAPK has an inhibitory effect on tumorigenesis (55, 56) and that a variety of agents, such as gemcitabine (5) and cisplatin (20), can also induce activation of p38 MAPK and internalization of EGFR into endosomal vesicles. Moreover, it has previously been reported that the Ser-1046/7 phosphorylation sites act to suppress the oncogenic signal transduction by the wild-type EGFR (21, 23). Hence, our present findings might provide a new therapeutic strategy for human colon cancer, although further investigations are necessary to elucidate the mechanism underlying EGFR down-regulation via its phosphorylation at serine residues.

Regarding our concern of how these findings would be translated into the clinic, the current limitation of the present study is the lack of practical tools to deliver UV-C irradiation onto the colon cancer tissue in the human body. Our hypothetical approaches would include a combination of extracorporeal generator and fiberscopic transmission of UV-C through colon endoscope or possible expansion of light emitting diode technique to exert shorter wavelength UV-C than with the currently available UV-A light emitting diode. However, substantial technical advances and some related time would be essentially required before practical application of UV-C for colon cancer management. Moreover, further studies are required to determine whether these effects of UV-C safely occur *in vivo*.

In summary, we found that UV-C induces EGFR down-regulation via p38 MAPK-mediated EGFR phosphorylation at Ser-1046/7. Moreover, our results strongly suggest that UV-C irradiation induces the removal of EGFR from cell surfaces that can evade colon cancer cells from oncogenic stimulation of EGF, resulting in cell cycle arrest in colon cancer cells.

Acknowledgment—We are very grateful to Yoko Kawamura for skillful technical assistance.

REFERENCES

1. Rusch, V., Klimstra, D., Venkatraman, E., Pisters, P. W., Langenfeld, J., and Dmitrovsky, E. (1997) *Clin. Cancer Res.* **3,** 515–522
2. Masuda, M., Suzui, M., and Weinstein, I. B. (2001) *Clin. Cancer Res.* **7,** 4220–4229
3. Fong, C. J., Sherwood, E. R., Mendelsohn, J., Lee, C., and Kozlowski, J. M. (1992) *Cancer Res.* **52,** 5887–5892
4. Pianetti, S., Guo, S., Kavanagh, K. T., and Sonenshein, G. E. (2002) *Cancer Res.* **62,** 652–655
5. Feng, F. Y., Varambally, S., Tomlins, S. A., Chun, P. Y., Lopez, C. A., Li, X., Davis, M. A., Chinnaiyan, A. M., Lawrence, T. S., and Nyati, M. K. (2007) *Oncogene* **26,** 3431–3439
6. Shimizu, M., Deguchi, A., Lim, J. T., Moriwaki, H., Kopelovich, L., and Weinstein, I. B. (2005) *Clin. Cancer Res.* **11,** 2735–2746
7. Meisenhelder, J., Suh, P. G., Rhee, S. G., and Hunter, T. (1989) *Cell* **57,** 1109–1122
8. Lowenstein, E. J., Daly, R. J., Batzer, A. G., Li, W., Margolis, B., Lammers, R., Ullrich, A., Skolnik, E. Y., Bar-Sagi, D., and Schlessinger, J. (1992) *Cell* **70,** 431–442
9. Rozakis-Adcock, M., McGlade, J., Mbamalu, G., Pelicci, G., Daly, R., Li, W., Batzer, A., Thomas, S., Brugge, J., Pelicci, P. G., Schlessinger, J., and Pawson, T. (1992) *Nature* **360,** 689–692
10. Levkowitz, G., Waterman, H., Ettenberg, S. A., Katz, M., Tsygankov, A. Y., Alroy, I., Lavi, S., Iwai, K., Reiss, Y., Ciechanover, A., Lipkowitz, S., and Yarden, Y. (1999) *Mol. Cell* **4,** 1029–1040
11. Zandi, R., Larsen, A. B., Andersen, P., Stockhausen, M. T., and Poulsen, H. S. (2007) *Cell Signal* **19,** 2013–2023
12. Arteaga, C. L. (2002) *Oncologist* **7,** (Suppl. 4) 31–39
13. Milano, G., Spano, J. P., and Leyland-Jones, B. (2008) *Br. J. Cancer* **99,** 1–5
14. Massie, C., and Mills, I. G. (2006) *Nat. Rev. Cancer* **6,** 403–409
15. Wiley, H. S. (2003) *Exp. Cell Res.* **284,** 78–88
16. Di Fiore, P. P., and De Camilli, P. (2001) *Cell* **106,** 1–4
17. McPherson, P. S., Kay, B. K., and Hussain, N. K. (2001) *Traffic* **2,** 375–384
18. Jaramillo, M. L., Leon, Z., Grothe, S., Paul-Roc, B., Abulrob, A., and O'Connor McCourt, M. (2006) *Exp. Cell Res.* **312,** 2778–2790
19. Khan, E. M., Heidinger, J. M., Levy, M., Lisanti, M. P., Ravid, T., and Goldkorn, T. (2006) *J. Biol. Chem.* **281,** 14486–14493
20. Winograd-Katz, S. E., and Levitzki, A. (2006) *Oncogene* **25,** 7381–7390
21. Countaway, J. L., McQuilkin, P., Gironès, N., and Davis, R. J. (1990) *J. Biol. Chem.* **265,** 3407–3416
22. Countaway, J. L., Nairn, A. C., and Davis, R. J. (1992) *J. Biol. Chem.* **267,** 1129–1140
23. Theroux, S. J., Latour, D. A., Stanley, K., Raden, D. L., and Davis, R. J. (1992) *J. Biol. Chem.* **267,** 16620–16626
24. Adachi, S., Shimizu, M., Shirakami, Y., Yamauchi, J., Natsume, H., Matsushima-Nishiwaki, R., To, S., Weinstein, I. B., Moriwaki, H., and Kozawa, O. (2009) *Carcinogenesis* **30,** 1544–1552
25. Adachi, S., Natsume, H., Yamauchi, J., Matsushima-Nishiwaki, R., Joe, A. K., Moriwaki, H., and Kozawa, O. (2009) *Cancer Lett.* **277,** 108–113
26. Adachi, S., Yasuda, I., Nakashima, M., Yamauchi, T., Yamauchi, J., Natsume, H., Moriwaki, H., and Kozawa, O. (2010) *Oncol. Rep.* **23,** 1709–1714
27. Habiro, A., Tanno, S., Koizumi, K., Izawa, T., Nakano, Y., Osanai, M., Mizukami, Y., Okumura, T., and Kohgo, Y. (2004) *Biochem. Biophys. Res. Commun.* **316,** 71–77
28. Koizumi, K., Tanno, S., Nakano, Y., Habiro, A., Izawa, T., Mizukami, Y., Okumura, T., and Kohgo, Y. (2005) *Anticancer Res.* **25,** 3347–3353
29. Latonen, L., and Laiho, M. (2005) *Biochim. Biophys. Acta* **1755,** 71–89
30. Zwang, Y., and Yarden, Y. (2006) *EMBO J.* **25,** 4195–4206
31. Nakashima, M., Adachi, S., Yasuda, I., Yamauchi, T., Kozawa, O., and Moriwaki, H. (2010) *Int. J. Oncol.* **36,** 585–592
32. Adachi, S., Nagao, T., To, S., Joe, A. K., Shimizu, M., Matsushima-Nishiwaki, R., Kozawa, O., Moriwaki, H., Maxfield, F. R., and Weinstein, I. B. (2008) *Carcinogenesis* **29,** 1986–1993
33. Adachi, S., Nagao, T., Ingolfsson, H. I., Maxfield, F. R., Andersen, O. S., Kopelovich, L., and Weinstein, I. B. (2007) *Cancer Res.* **67,** 6493–6501
34. Blumenthal, R. D., and Goldenberg, D. M. (2007) *Mol. Biotechnol.* **35,** 185–197
35. Sherr, C. J. (1996) *Science* **274,** 1672–1677
36. Rice, P. L., Washington, M., Schleman, S., Beard, K. S., Driggers, L. J., and Ahnen, D. J. (2003) *Cancer Res.* **63,** 616–620
37. Oksvold, M. P., Huitfeldt, H. S., Østvold, A. C., and Skarpen, E. (2002) *J. Cell Sci.* **115,** 793–803
38. Cuenda, A., Rouse, J., Doza, Y. N., Meier, R., Cohen, P., Gallagher, T. F., Young, P. R., and Lee, J. C. (1995) *FEBS Lett.* **364,** 229–233
39. Bain, J., Plater, L., Elliott, M., Shpiro, N., Hastie, C. J., McLauchlan, H., Klevernic, I., Arthur, J. S., Alessi, D. R., and Cohen, P. (2007) *Biochem. J.* **408,** 297–315
40. Alessi, D. R., Cuenda, A., Cohen, P., Dudley, D. T., and Saltiel, A. R. (1995) *J. Biol. Chem.* **270,** 27489–27494
41. Bennett, B. L., Sasaki, D. T., Murray, B. W., O'Leary, E. C., Sakata, S. T., Xu,

W., Leisten, J. C., Motiwala, A., Pierce, S., Satoh, Y., Bhagwat, S. S., Manning, A. M., and Anderson, D. W. (2001) *Proc. Natl. Acad. Sci. U.S.A.* **98,** 13681–13686
42. Yamaguchi, K., Shirakabe, K., Shibuya, H., Irie, K., Oishi, I., Ueno, N., Taniguchi, T., Nishida, E., and Matsumoto, K. (1995) *Science* **270,** 2008–2011
43. Ninomiya-Tsuji, J., Kishimoto, K., Hiyama, A., Inoue, J., Cao, Z., and Matsumoto, K. (1999) *Nature* **398,** 252–256
44. Wang, C., Deng, L., Hong, M., Akkaraju, G. R., Inoue, J., and Chen, Z. J. (2001) *Nature* **412,** 346–351
45. Moriguchi, T., Kuroyanagi, N., Yamaguchi, K., Gotoh, Y., Irie, K., Kano, T., Shirakabe, K., Muro, Y., Shibuya, H., Matsumoto, K., Nishida, E., and Hagiwara, M. (1996) *J. Biol. Chem.* **271,** 13675–13679
46. Hammaker, D. R., Boyle, D. L., Inoue, T., and Firestein, G. S. (2007) *Arthritis Res. Ther.* **9,** R57
47. Dérijard, B., Raingeaud, J., Barrett, T., Wu, I. H., Han, J., Ulevitch, R. J., and Davis, R. J. (1995) *Science* **267,** 682–685
48. Henson, E. S., and Gibson, S. B. (2006) *Cell Signal.* **18,** 2089–2097
49. Cheng, J. Q., Lindsley, C. W., Cheng, G. Z., Yang, H., and Nicosia, S. V. (2005) *Oncogene* **24,** 7482–7492
50. Rogakou, E. P., Boon, C., Redon, C., and Bonner, W. M. (1999) *J. Cell Biol.* **146,** 905–916
51. Norval, M. (2001) *J. Photochem. Photobiol. B* **63,** 28–40
52. Matsuzawa, A., and Ichijo, H. (2001) *J. Biochem.* **130,** 1–8
53. Rosette, C., and Karin, M. (1996) *Science* **274,** 1194–1197
54. Levkowitz, G., Waterman, H., Zamir, E., Kam, Z., Oved, S., Langdon, W. Y., Beguinot, L., Geiger, B., and Yarden, Y. (1998) *Genes Dev.* **12,** 3663–3674
55. Lavoie, J. N., L'Allemain, G., Brunet, A., Müller, R., and Pouysségur, J. (1996) *J. Biol. Chem.* **271,** 20608–20616
56. Kennedy, N. J., Cellurale, C., and Davis, R. J. (2007) *Cancer Cell* **11,** 101–103

Biochemical and Biophysical Research Communications 414 (2011) 53–59

Contents lists available at SciVerse ScienceDirect

Biochemical and Biophysical Research Communications

journal homepage: www.elsevier.com/locate/ybbrc

Ultraviolet enhances the sensitivity of pancreatic cancer cells to gemcitabine by activation of 5′ AMP-activated protein kinase

Seiji Adachi [a,b,*], Ichiro Yasuda [a], Junji Kawaguchi [a], Takahiro Yamauchi [a], Masanori Nakashima [a], Masahiko Itani [b], Momoko Nakamura [b], Takashi Yoshioka [b], Hisataka Moriwaki [a], Osamu Kozawa [b]

[a] Department of Gastroenterology, Gifu University Graduate School of Medicine, Gifu 501-1194, Japan
[b] Department of Pharmacology, Gifu University Graduate School of Medicine, Gifu 501-1194, Japan

ARTICLE INFO

Article history:
Received 1 September 2011
Available online 10 September 2011

Keywords:
Pancreatic cancer
Combination
UV-C
Gemcitabine
AMPK

ABSTRACT

Although gemcitabine is recognized as the standard drug for the treatment of advanced pancreatic cancer, the clinical outcome is not satisfactory. We recently reported that relatively high dose ultraviolet-C (UV-C; 200 J) inhibits cell growth by desensitization of epidermal growth factor receptor (EGFR) in human pancreatic cancer cells. In the present study, we investigated the combination effects of low dose UV-C (10 J) and gemcitabine on apoptosis and cell growth in these cells. UV-C enhanced gemcitabine-induced suppression of cell viability. In addition, the combination use clearly induced apoptosis, while neither UV-C nor gemcitabine alone did. Concurrently, combination use caused the decrease in the EGFR protein level and reduced EGF-induced activation of Akt pathway, subsequently resulting in accumulation of β-catenin. The order of the treatment with UV-C and gemcitabine did not affect their synergistic effects on apoptosis and cell growth. Interestingly, combination use synergistically induced phosphorylation of 5′ AMP-activated protein kinase (AMPK) alpha at Thr172 and acetyl-CoA carboxylase at Ser79 as a downstream molecular target of AMPK. AMPK activator, 5-aminoimidazole-4-carboxamide-1-β-riboside, induced apoptosis and suppressed cell growth in these cells, thus suggesting that combination effects of UV-C and gemcitabine is due to the activation of AMPK. Together, our findings could provide a new aspect of pancreatic cancer therapy.

© 2011 Elsevier Inc. All rights reserved.

1. Introduction

Because of the difficulty in early diagnose of pancreatic cancer, most patients with this malignancy have already reached an advanced stage when the first symptoms appear. The standard treatment for advanced pancreatic cancer is chemotherapy. Gemcitabine is a nucleoside analogue of deoxycytidine that is enzymatically activated inside the cell where it subsequently inhibits DNA synthesis and induces apoptosis [1] and has been the first line drug for pancreatic cancer. However, the median survival of patients treated with gemcitabine is not satisfactory. Moreover, a number of studies have compared gemcitabine alone with gemcitabine-based combinations, such as fluorouracil, capecitabine, cisplatin, docetaxel, irinotecan, oxaliplatin, or pemetrexed, but they added no clear survival benefit [2]. Therefore, the breakthrough development of treatments for unresectable pancreatic cancer is required urgently.

The epidermal growth factor receptor (EGFR) is a member of the ErbB family of receptor tyrosine kinases [3]. Binding of ligands such as epidermal growth factor (EGF) to the EGFR leads to receptor dimerization and autophosphorylation [4]. The autophosphorylation of the EGFR at tyrosine residues activates downstream signalling, including Akt-glycogen synthase kinase (GSK)-3β pathway, thus resulting in the stimulation of cell proliferation [5]. The EGFR has been reported to be overexpressed in pancreatic cancer [6]. We have recently reported that the blockade of EGF stimulation significantly suppressed pancreatic cancer cell growth, suggesting that the EGFR pathway plays an important role in proliferation of these cells [7]. Therefore, EGFR-mediated pathways appear to be important potential targets for new therapies for this malignancy. Moreover, the addition of EGFR-targeted therapy to gemcitabine in advanced pancreatic cancer has been demonstrated to provide a small, but statistically significant, survival benefit [8].

Ultraviolet (UV) radiation from sunlight is sorted by wavelength regions: long-wavelength UV-A (320–400 nm), medium-wavelength UV-B (280–320 nm) and short-wavelength UV-C (200–280 nm). In general, UV-A and UV-B are recognized as the major carcinogenic components of sunlight [9], and UV-C is used for studying DNA damage and cellular DNA repair process, and commonly applied for equipments such as water sterilization. We recently reported that UV-C irradiation suppresses cell growth via downregulation of EGFR in human pancreatic cancer cells [10].

* Corresponding author at: Department of Gastroenterology, Gifu University Graduate School of Medicine, Gifu 501-1194, Japan. Fax: +81 58 230 6218.
E-mail address: seijiadachi0123@gmail.com (S. Adachi).

0006-291X/$ - see front matter © 2011 Elsevier Inc. All rights reserved.
doi:10.1016/j.bbrc.2011.09.020

Moreover, our recent study shows that UV-C can induce evasion of colon cancer cells from oncogenic stimulation of EGF [11]. Hence, UV-C might be applied for clinical strategy against human cancers.

5′ AMP-activated protein kinase (AMPK) is a central cellular energy sensor which may be a crucial factor in the interaction between metabolism and cancer [12]. AMPK activation results in the restoration of energy levels through regulation of metabolism and growth [13], and the loss of AMPK activity causes cell proliferation, suggesting that AMPK is a potential target for anti-cancer therapy. In this study, we tried the combination use of low dose UV-C and gemcitabine in pancreatic cancer cells and found that this exerts synergistic effects on the induction of apoptosis and suppression of cell growth via activation of AMPK.

2. Materials and methods

2.1. Materials

Gemcitabine was obtained from Eli Lilly Co. (Indianapolis, IN, USA) and 5-aminoimidazole-4-carboxamide-1-β-riboside (AICAR) was obtained from Calbiochem-Novabiochem Co. (La Jolla, CA, USA). EGF was purchased from Sigma Chemical Co. (St. Louis, MO, USA). Antibodies against EGFR and glyceraldehyde-3-phosphate dehydrogenase (GAPDH) were obtained from Santa Cruz Biotechnology (Santa Cruz, CA, USA). Other antibodies were purchased from Cell Signalling (Beverly, MA, USA). 3-(4,5-dimethylthiazol-2-yl)-2,5-diphenyltetra-zolium bromide (MTT) cell proliferation kit I and Cell Proliferation ELISA (BrdU) were obtained from Roche Diagnostics Co. (Indianapolis, IN, USA).

2.2. Cell culture

Panc1 and KP3 pancreatic cancer cells were provided from American Type Culture Collection (Manassas, VA, USA). They were grown in Roswell Park Memorial Institute (RPMI) 1640 (Invitrogen, San Diego, CA, USA) supplemented with 10% heat-inactivated fetal calf serum (FCS), penicillin (100 U/ml) and streptomycin (100 μg/ml) in a humidified 5% CO_2 incubator at 37 °C.

2.3. UV-C exposure

UV-C exposure to cells was performed in UVC 500 UV Crosslinker (GE Healthcare) with 0–500 J/m^2 (J) UV at 254 nm. After aspiration of the growth medium, the cells were exposed to UV-C (0 or 10 J) and then incubated in the growth medium for the indicated periods.

2.4. Cell viability assay and BrdU incorporation assay

In cell viability assay, the cells (5×10^3/well) were seeded onto 96-well plates and 24 h later, the cells were exposed to 10 J of UV-C and/or gemcitabine at the indicated concentrations. These cells were then incubated in RPMI for 48 h and the remaining cells were finally counted by MTT cell proliferation kit. For the latter assay, the cells (7×10^3/well) were seeded onto 96-well plates and 48 h later, the cells were exposed to 10 J of UV-C and/or 10 μM of gemcitabine or 10 mM of AICAR. These cells were then incubated in RPMI without FCS for 48 h. BrdU incorporation was finally measured using Cell Proliferation ELISA. All assays were done at least in triplicate.

2.5. Western blot analysis

The cells were lysed in lysis buffer and were examined by Western blot analysis as previously described [14].

2.6. Immunofluorescence microscopy

Immunofluorescence microscopy was performed as described previously [15]. The cells were first exposed to UV-C (10 J) and incubated for 24 h at 37 °C, followed by exposure to Hoechst 33258 (Wako, Tokyo, Japan) for 30 min. The cells were then examined by fluorescence microscopy, BIOREVO (BZ-9000) (Keyence, Tokyo, Japan).

2.7. Image analysis

The protein band intensities in the Western blot analysis were determined by integrating the optical density over the band area (band volume) using the NIH image software program (Image J ver. 1.32). Based on the intensity of the control protein band on the X-ray film, the protein samples were quantitatively compared.

3. Results

UV-C enhanced gemcitabine-induced cytotoxicity in Panc1 and KP3 pancreatic cancer cells

As shown in Fig. 1A, 10 μM of gemcitabine alone for 48 h caused approximately 20% reduction in cell viability and only 30% reduction was seen even when the cells were treated with 100 μM of gemcitabine alone in KP3 cells (Fig. 1A). However, pretreatment with UV-C significantly increased gemcitabine-induced cytotoxicity in KP3 cells, while 10 J of UV-C alone did not affect KP3 cell viability (Fig. 1A). Ten μM and 30 μM of gemcitabine combined with UV-C caused 50% and 75% reduction in cell viability in KP3 cells, respectively. As well, we used another pancreatic cancer cell line, Panc1, and observed similar effect to that in KP3 cells (Fig. 1B). These results suggest that UV-C enhances gemcitabine-induced suppression of cell viability in pancreatic cancer cells.

3.1. Combination use of UV-C and gemcitabine induced apoptosis in pancreatic cancer cells

In order to elucidate how UV-C enhances gemcitabine-induced suppression of cell viability, we next examined the effects of UV-C and gemcitabine on cell apoptosis in KP3 cells. Apoptotic cells are easily detected by the Hoechst 33258 staining. In addition, PARP helps cells to maintain their viability, while cleavage of PARP induces apoptosis. In Fig. 1C, while 10 J of UV-C alone as well as 10 μM of gemcitabine alone slightly increased the number of Hoechst 33258-positive cells in KP3 cells, combination use caused a marked increase in the number of those cells (Fig. 1C). Similarly, while either UV-C or gemcitabine alone did not induce PARP cleavage, this was clearly observed when the cells were treated with both UV-C and gemcitabine (Fig. 1D). These results suggest that synergistic effect of UV-C and gemcitabine on the suppression of cell viability is, at least in part, due to the induction of cell apoptosis.

3.2. UV-C enhanced gemcitabine-induced cell growth suppression in pancreatic cancer cells

As depicted in Fig. 2A, UV-C had little effect on BrdU incorporation and 10 μM of gemcitabine alone caused a slight suppression of its incorporation (Fig. 2A). As expected, when the cells were exposed to UV-C and then treated with gemcitabine for 48 h, BrdU incorporation was significantly suppressed ($p = 0.0047$), compared with gemcitabine-treated cells (Fig. 3A). We recently reported that the EGFR pathway plays an important role in pancreatic cancer cell proliferation [7]. Therefore, we next examined the effect of UV-C and gemcitabine on the protein level of EGFR in KP3 cells. In Fig. 2B, whereas either UV-C or gemcitabine had little effect on

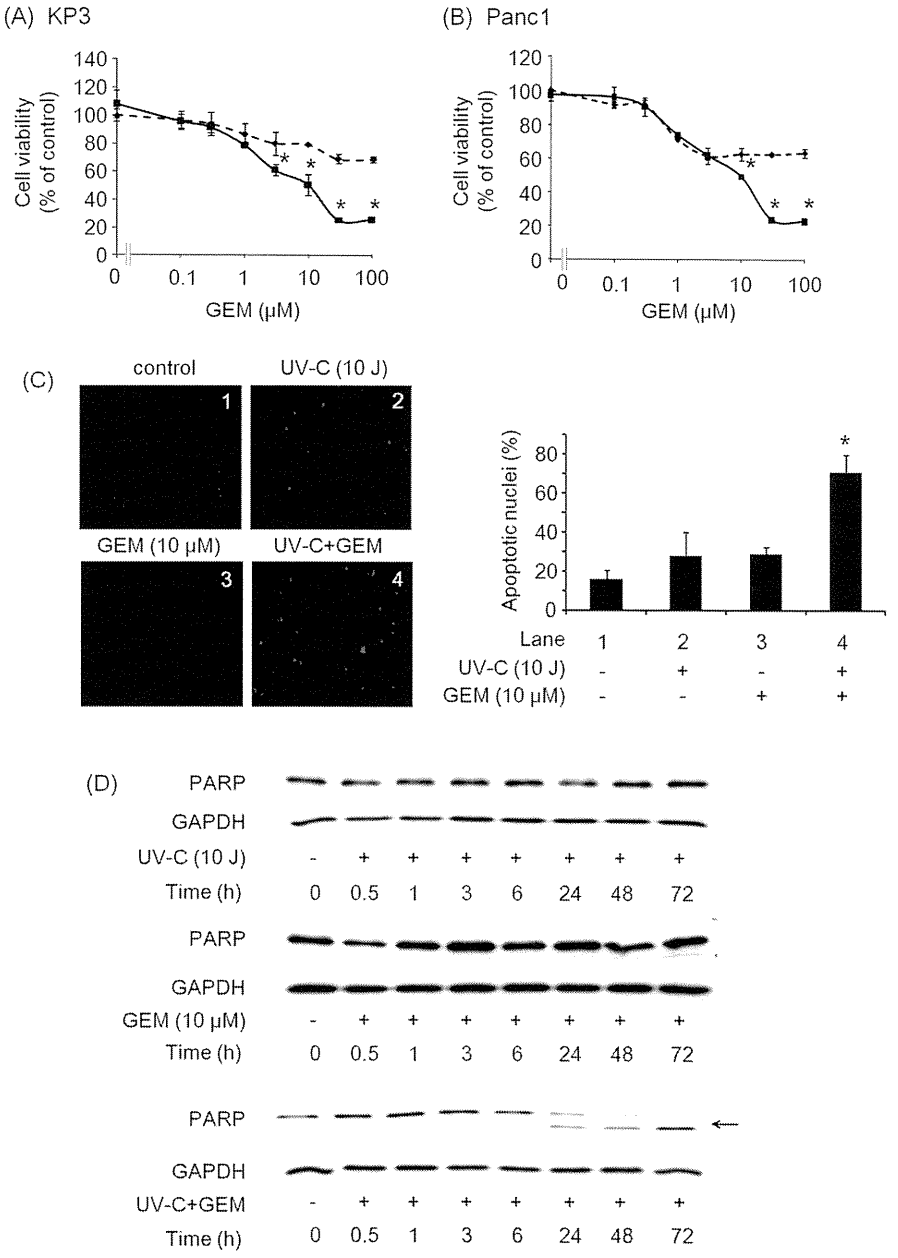

Fig. 1. (A and B) UV-C enhanced the inhibition of cell growth by gemcitabine in pancreatic cancer cells. The KP3 (A) and Panc1 (B) cells were first exposed to UV-C (0 or 10 J) and then incubated with gemcitabine (GEM; 0–100 μM) for 48 h. Cell viability assay was then performed using the MTT cell proliferation kit I. Results are expressed as percentage of growth with 100% representing untreated control cells. Bars designate SD of triplicate assays. Broken line: GEM alone; solid line: UV-C + GEM. (C) The combination use of UV-C and GEM induced DNA fragmentation in KP3 cells. The KP3 cells were first exposed to UV-C (0 or 10 J) and then incubated with or without 10 μM of GEM for 48 h. They were then exposed to Hoechst 33258 (blue signal) and were examined by fluorescence microscopy. The numbers of Hoechst 33258-positive cells (apoptotic nuclei) from five randomly chosen fields (×40) were counted, respectively. Bars designate SD of triplicate assays. The asterisk indicates significant difference ($p < 0.05$), as compared with the cells treated with GEM alone (lane 3). (D) The combination use of UV-C and GEM induced PARP cleavage in KP3 cells. The KP3 cells were first exposed to UV-C (0 or 10 J) and then incubated with or without gemcitabine 10 μM of GEM for the indicated periods. Protein extracts were then harvested and examined by Western blotting using antibodies against PARP and GAPDH. The arrow indicates cleaved PARP.

the EGFR protein level, combination use markedly decreased EGFR level (Fig. 2B). Therefore, it seems that cell growth suppression by combination use of UV-C and gemcitabine is due to the decrease in EGFR protein level.

3.3. Combination use of UV-C and gemcitabine suppressed EGF-induced activation of Akt-GSK-3β pathway in pancreatic cancer cells

Through EGF-binding to cell surface EGFR, it activates an extensive network of signal transduction pathways including the Akt pathways, which regulates multiple biological processes including survival, proliferation, and cell growth [16]. Therefore, we next examined the effect of UV-C and gemcitabine on EGF-induced phosphorylation of Akt in KP3 cells. EGF induced phosphorylation of Akt within 5 min and this was decreased thereafter (Fig. 2C). UV-C and gemcitabine alone slightly suppressed EGF-induced phosphorylation of Akt (Fig. 2C). Moreover, the combination use markedly suppressed EGF-induced phosphorylation of Akt (Fig. 3C). GSK-3β is a critical downstream element of the Akt pathway, and its activity can be inhibited by Akt-mediated phosphory-

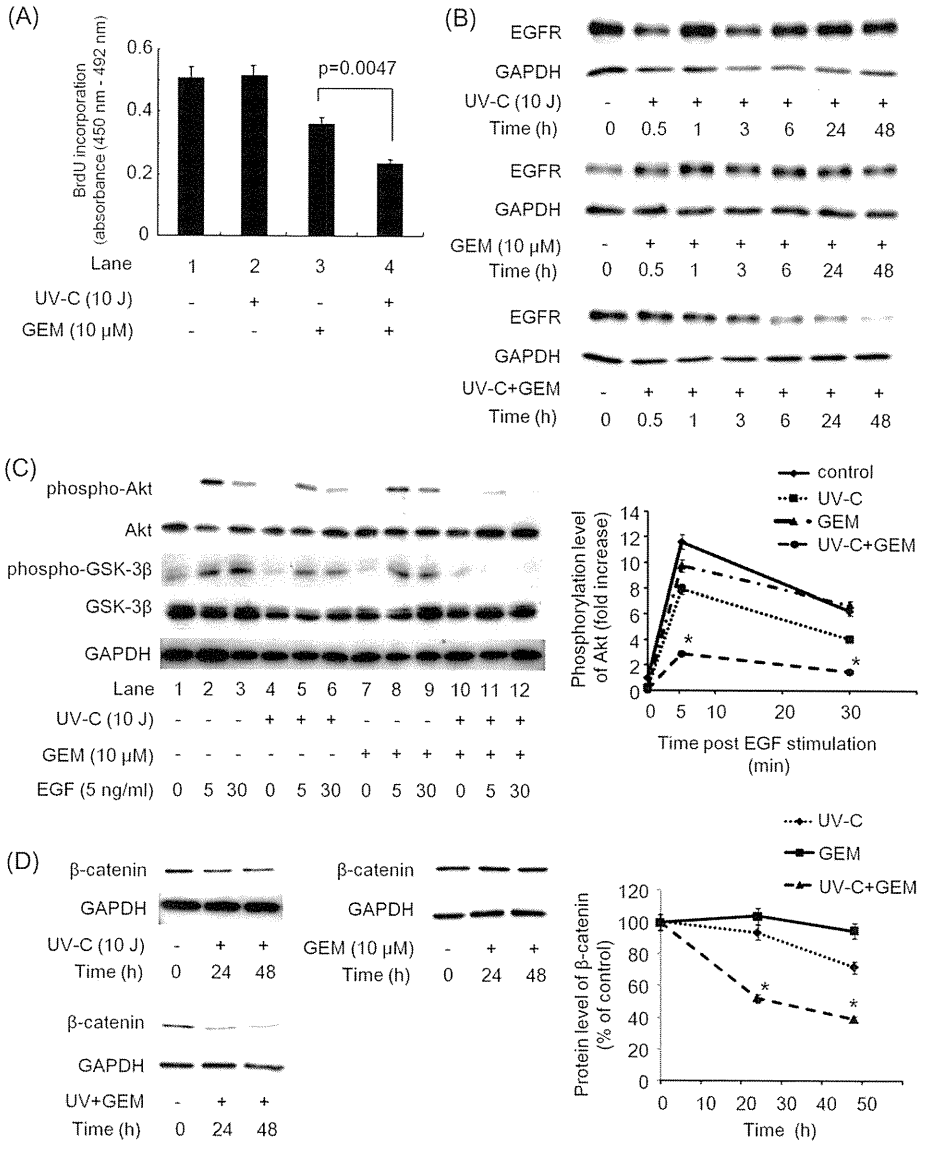

Fig. 2. (A) The combination use of UV-C and gemcitabine (GEM) inhibited BrdU incorporation in KP3 cells. The KP3 cells were first exposed to UV-C (0 or 10 J) and then incubated with or without 10 μM of GEM for 48 h and the measurement of BrdU incorporation during DNA synthesis were performed using cell proliferation ELISA (BrdU). Results are expressed as the absorbance (OD 405 nm–492 nm). Bars designate SD of triplicate assays. The asterisk indicates significant difference ($p = 0.0047$), between the indicated pairs. (B) The combination use of UV-C and GEM caused the decrease in the EGFR protein level in KP3 cells. The KP3 cells were first exposed to UV-C (0 or 10 J) and then incubated with or without 10 μM of GEM for the indicated periods. Protein extracts were then harvested and examined by Western blotting using antibodies against EGFR and GAPDH. (C) The combination use of UV-C and GEM suppressed EGF-induced Akt pathway in KP3 cells. The KP3 cells were first exposed to UV-C (0 or 10 J) and then incubated with or without 10 μM of GEM for 24 h. They were then stimulated with EGF (5 ng/ml) for the indicated periods. Protein extracts were then harvested and examined by Western blotting using antibodies against phospho-Akt, Akt, phospho-GSK3β, GSK3β and GAPDH. Right line graph shows the quantification data for the relative phosphorylation levels of Akt, after normalization with respect to total Akt, as determined by densitometry. Bars designate SD of triplicate assays. $^*p < 0.05$: compared to the cells treated with GEM alone. (D) The combination use of UV-C and GEM caused the decrease in the β-catenin protein level in KP3 cells. The KP3 cells were first exposed to UV-C (0 or 10 J) and then incubated with or without 10 μM of GEM for the indicated periods. Protein extracts were then harvested and examined by Western blotting using antibodies against β-catenin and GAPDH. Right line graph shows the quantification data for the relative levels of β-catenin, after normalization with respect to GAPDH, as determined by densitometry. Bars designate SD of triplicate assays. $^*p < 0.05$: compared to the cells treated with GEM alone.

lation of GSK-3β at Ser9 [17]. As expected, EGF failed to phosphorylate GSK-3β at Ser9 in the cells treated with UV-C and gemcitabine (Fig. 3C).

Deregulation of Wnt-β-catenin cascades has been reported in many types of cancers, including pancreatic cancer [18] and phosphorylated form of GSK-3β caused the accumulation of β-catenin. As shown in Fig. 2D, combination use of UV-C and gemcitabine caused the decrease in the protein level of β-catenin, whereas either UV-C or gemcitabine alone failed to affect. Together, our results suggest that combination use of UV-C and gemcitabine induces the suppressive effect on cell growth, at least in part, by inhibiting the Akt pathway.

3.4. The order of the treatment with UV-C and gemcitabine did not affect their synergistic effects on apoptosis and cell growth

We next examined which is more effective treatment to enhance the sensitivity to gemcitabine, pre- or post-treatment with UV-C. Either gemcitabine or UV-C did not affect the protein level of EGFR as well as cleavage of PARP (Fig. 3A). When the cells were

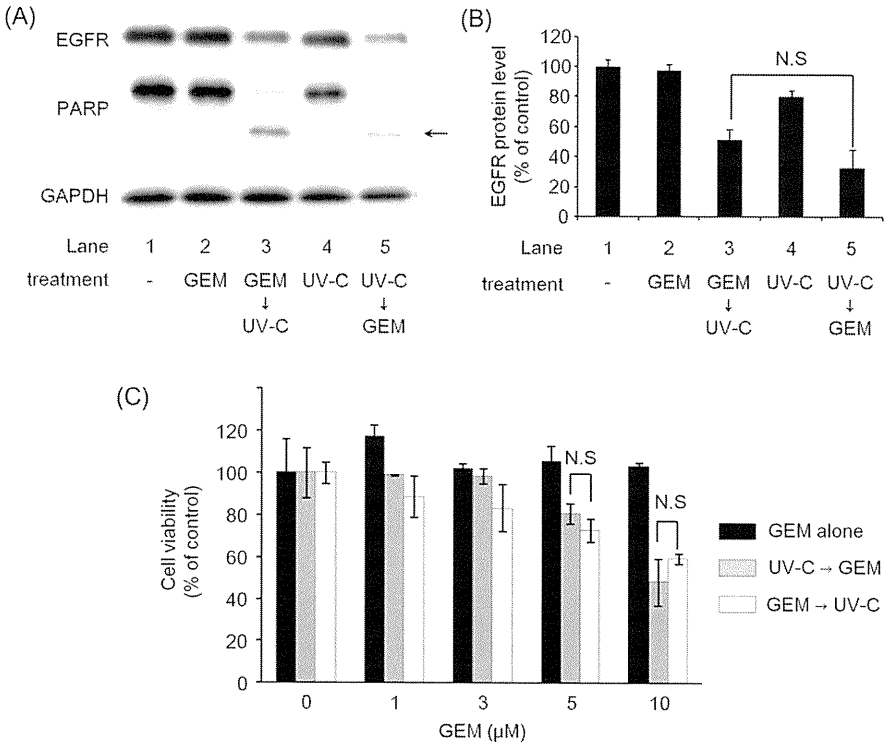

Fig. 3. The order of treatment with UV-C and gemcitabine (GEM) is not critical for their combination effect in KP3 cells. (A) The cells (lanes 4 and 5) were exposed to 10 J of UV-C and then treated with (lane 5) or without (lane 4) GEM (10 μM) for 8 h. The media were then exchanged to the fresh one and incubated for another 40 h. The other cells were first treated with (lanes 2 and 3) or without (lane 1) GEM (10 μM) for 8 h and then exposed to 10 J of UV-C (lane 3) or not (lanes 1 and 2), and subsequent incubation for another 40 h in the fresh media. Protein extracts were then harvested and examined by Western blotting using antibodies against EGFR, PARP and GAPDH. The arrow indicates cleaved PARP. (B) The bar graph shows the quantification data for the relative levels of EGFR after normalization with respect to GAPDH, as determined by densitometry. Bars designate SD of triplicate assays. No significant difference exists between the indicated pairs. (C) Some cells (grey bar) were first exposed to 10 J of UV-C and then treated with GEM at the indicated concentrations for 8 h. The media were then exchanged to the fresh one and incubated for another 40 h. The other cells (black and white bars) were first treated with GEM at the indicated concentrations for 8 h and then exposed to 10 J of UV-C (white bar) or not (black bar), and subsequent incubation for another 40 h in the fresh media. Cell viability assay was then performed using the MTT cell proliferation kit I. Results are expressed as percentage of growth with 100% representing untreated control cells. Bars designate SD of triplicate assays.

pretreated with gemcitabine for 8 h and then exposed to UV-C (gemcitabine → UV-C treatment), we observed the decrease in EGFR protein level in addition to the induction of PARP cleavage, which are similar to the results obtained from UV-C → gemcitabine treatment (Fig. 3A and B). Moreover, similar results were observed in cell viability assay (Fig. 3C). Taken together, our findings strongly suggest that the order is not important for combination use of UV-C and gemcitabine.

3.5. The combination use of UV-C and gemcitabine induced activation of AMPKα in pancreatic cancer cells

In order to investigate the mechanism underlying combination effects of UV-C and gemcitabine, we next examined several kinase cascades including AMPK. Interestingly, whereas either UV-C or gemcitabine had little effect on phosphorylation of AMPKα (Thr172) and acetyl-CoA carboxylase (ACC; Ser 79) as a downstream molecular target of AMPK, the combination use caused a marked phosphorylation of both proteins (Fig. 4A). These results led us to speculate that activation of AMPK induced by UV-C and gemcitabine exert anti-cancer effect, such as the induction of apoptosis and the suppression of cell growth.

To verify these findings, we used AMPK activator, AICAR and found that increasing doses of AICAR caused cleavage of PARP (Fig. 4B) and this increased Hoechst 33258-positive cells (Fig. 4C), suggesting that activation of AMPK leads to apoptosis in pancreatic cancer cells. Moreover, since AICAR suppressed BrdU incorporation (Fig. 4D), indicating that activation of AMPK inhibits cell cycle. Taken together with the results shown above, it is most likely that the synergistic effects of UV-C and gemcitabine are exerted through the activation of AMPK.

4. Discussion

We have recently reported the availability of UV-C for the treatment of human pancreatic cancers [10]. In that article, we used relatively high dose UV-C (200 J), and showed that UV-C has a suppressive effect on cell proliferation in pancreatic cancer cells, but not normal pancreas epithelial cells. In the present study, we demonstrated the synergistic effects of low dose UV-C (10 J) and gemcitabine. First, we showed that UV-C enhanced gemcitabine-induced cytotoxicity in Panc1 and KP3 cells (Fig. 1A and B). This combination use caused cell apoptosis (Fig. 1C and D) as well as inhibition of cell proliferation (Fig. 2A), concurrent with downregulation of EGFR which exerts oncogenic signalling, such as the Akt pathway (Fig. 2B–D). These results indicate that the synergistic effect against pancreatic cancer cells on cell viability is due to the induction of cell apoptosis and suppression of cell proliferation.

Gemcitabine is now regarded as the first-line agent for advanced pancreatic cancer, but the median survival time of patients treated with gemcitabine is not satisfactory. Importantly, it has been reported that gemcitabine induces cell apoptosis by activating p38 mitogen-activated protein kinase (MAPK) in PK-1 and PCI-43 human pancreatic cancer cell lines [19]. However, in this study, the combination use of UV-C and gemcitabine did not induce phosphorylation of p38 MAPK in Panc1 and KP3 cells (data not shown). Therefore, it is likely that the synergistic effect of UV-C and gemcitabine is independent of the p38 MAPK pathway.

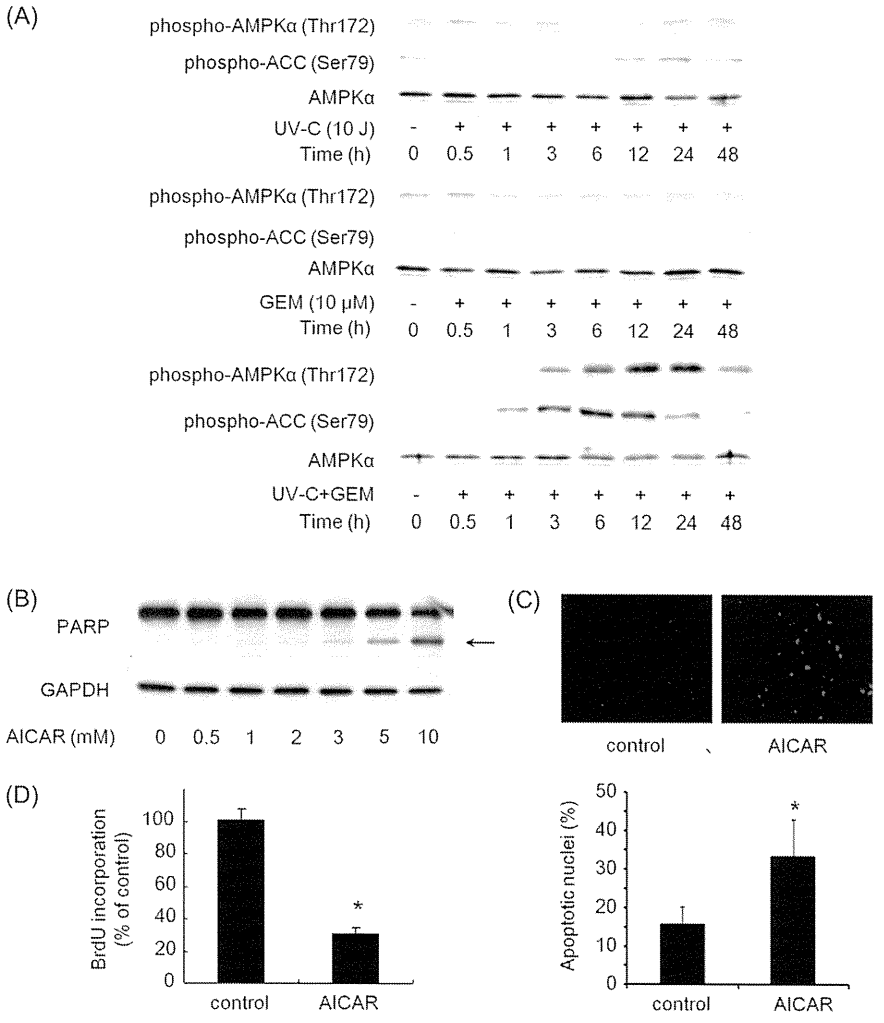

Fig. 4. (A) The combination use of UV-C and gemcitabine (GEM) caused the activation of AMPK in KP3 cells. The KP3 cells were first exposed to UV-C (0 or 10 J) and then incubated with or without 10 μM of GEM for the indicated periods. Protein extracts were then harvested and examined by Western blotting using antibodies against phospho-AMPKα (Thr172), phospho-acetyl-CoA carboxylase (ACC; Ser79) and AMPKα. (B) AMPK activator, AICAR, induced apoptosis in KP3 cells. The KP3 cells were treated with AICAR at the indicated concentrations for 24 h. Protein extracts were then harvested and examined by Western blotting using antibodies against PARP and GAPDH. The arrow indicates cleaved PARP. (C) The KP3 cells were treated with 10 mM of AICAR for 24 h and were then exposed to Hoechst 33258 (blue signal) and were examined by fluorescence microscopy. The numbers of Hoechst 33258-positive cells (apoptotic nuclei) from five randomly chosen fields (×40) were counted, respectively. Bars designate SD of triplicate assays. The asterisk indicates significant difference ($p < 0.05$), as compared with the control cells. (D) The KP3 cells were treated with 10 mM of AICAR for 24 h and the measurement of BrdU incorporation during DNA synthesis were performed using cell proliferation ELISA (BrdU). Results are expressed as the absorbance (OD 405 nm–492 nm). Bars designate SD of triplicate assays. The asterisk indicates significant difference ($p < 0.05$), as compared with the control cells.

AMPK is a serine/threonine protein kinase, which serves as an energy sensor in eukaryotic cell types. Increasing evidence shows that AMPK activation strongly suppresses cell proliferation in normal cells as well as in cancer cells, indicating that AMPK functions as a suppressor of cell proliferation by controlling a variety of cellular events in these cells [20]. Metformin, which is widely used as an anti-diabetic drug, has been recently reported to be associated with a reduced risk of cancer associated with insulin resistance [12,21]. The effects of metformin are explained by the activation of AMPK, which regulates cellular energy metabolism [22]. Of interest, in the present study, the combination use of UV-C and gemcitabine induced activation of AMPK (Fig. 4A). The order of the treatment with UV-C and gemcitabine is not critical for their combination effect (Fig. 3). Moreover, we observed the activation of AMPK in the cells, which were first treated with gemcitabine for 8 h and then exposed to UV-C, subsequent incubation for another 40 h (data not shown), consistently with the results shown in Fig. 3. However, further investigation is necessary to elucidate how the combination use of UV-C and gemcitabine activates AMPK.

In summary, we presented that UV-C enhances the sensitivity to gemcitabine in pancreatic cancer cells via activation of AMPK. Our novel findings could provide a fresh development for human pancreatic cancer therapy, although the development of devices that supply UV-C efficiently, for example with endoscopic approach, is also required for future clinical application.

Acknowledgment

We are very grateful to Yoko Kawamura for skillful technical assistance. This work was supported in part by Grant-in-Aid for Scientific Research (22790639 to S.A) from the Ministry of Education, Science, Sports and Culture of Japan.

References

[1] W. Plunkett, P. Huang, C.E. Searcy, V. Gandhi, Gemcitabine: preclinical pharmacology and mechanisms of action, Semin. Oncol. 23 (1996) 3–15.
[2] A. Stathis, M.J. Moore, Advanced pancreatic carcinoma: current treatment and future challenges, Nat. Rev. Clin. Oncol. 7 (2010) 163–172.

[3] J. Marshall, Clinical implications of the mechanism of epidermal growth factor receptor inhibitors, Cancer 107 (2006) 1207–1218.
[4] R. Zandi, A.B. Larsen, P. Andersen, M.T. Stockhausen, H.S. Poulsen, Mechanisms for oncogenic activation of the epidermal growth factor receptor, Cell. Signal. 19 (2007) 2013–2023.
[5] T. Lahusen, M. Fereshteh, A. Oh, A. Wellstein, A.T. Riegel, Epidermal growth factor receptor tyrosine phosphorylation and signaling controlled by a nuclear receptor coactivator, amplified in breast cancer 1, Cancer Res. 67 (2007) 7256–7265.
[6] K. Tobita, H. Kijima, S. Dowaki, H. Kashiwagi, Y. Ohtani, Y. Oida, H. Yamazaki, M. Nakamura, Y. Ueyama, M. Tanaka, S. Inokuchi, H. Makuuchi, Epidermal growth factor receptor expression in human pancreatic cancer: significance for liver metastasis, Int. J. Mol. Med. 11 (2003) 305–309.
[7] M. Nakashima, S. Adachi, I. Yasuda, T. Yamauchi, J. Kawaguchi, T. Hanamatsu, T. Yoshioka, Y. Okano, Y. Hirose, O. Kozawa, H. Moriwaki, Inhibition of Rho-associated coiled-coil containing protein kinase enhances the activation of epidermal growth factor receptor in pancreatic cancer cells, Mol. Cancer 10 (2011) 79.
[8] B.A. Faller, B. Burtness, Treatment of pancreatic cancer with epidermal growth factor receptor-targeted therapy, Biologics 3 (2009) 419–428.
[9] L. Latonen, M. Laiho, Cellular UV damage responses-functions of tumor suppressor p53, Biochim. Biophys. Acta 1755 (2005) 71–89.
[10] T. Yamauchi, S. Adachi, I. Yasuda, M. Nakashima, J. Kawaguchi, Y. Nishii, T. Yoshioka, Y. Okano, Y. Hirose, O. Kozawa, H. Moriwaki, UV-C irradiation induces downregulation of EGF receptor via phosphorylation at serine 1046/1047 in human pancreatic cancer cells. Radiat. Res. (in press).
[11] S. Adachi, I. Yasuda, M. Nakashima, T. Yamauchi, J. Kawaguchi, M. Shimizu, M. Itani, M. Nakamura, Y. Nishii, T. Yoshioka, Y. Hirose, Y. Okano, H. Moriwaki, O. Kozawa, Ultraviolet irradiation can induce evasion of colon cancer cells from stimulation of epidermal growth factor, J. Biol. Chem. 286 (2011) 26178–26187.
[12] M. Jalving, J.A. Gietema, J.D. Lefrandt, S. de Jong, A.K. Reyners, R.O. Gans, E.G. de Vries, Metformin: taking away the candy for cancer?, Eur J. Cancer 46 (2010) 2369–2380.
[13] M.C. Towler, D.G. Hardie, AMP-activated protein kinase in metabolic control and insulin signaling, Circ. Res. 100 (2007) 328–341.
[14] S. Adachi, T. Nagao, H.I. Ingolfsson, F.R. Maxfield, O.S. Andersen, L. Kopelovich, I.B. Weinstein, The inhibitory effect of (-)-epigallocatechin gallate on activation of the epidermal growth factor receptor is associated with altered lipid order in HT29 colon cancer cells, Cancer Res. 67 (2007) 6493–6501.
[15] S. Adachi, M. Shimizu, Y. Shirakami, J. Yamauchi, H. Natsume, R. Matsushima-Nishiwaki, S. To, I.B. Weinstein, H. Moriwaki, O. Kozawa, (-)-Epigallocatechin gallate downregulates EGF receptor via phosphorylation at Ser1046/1047 by p38 MAPK in colon cancer cells, Carcinogenesis 30 (2009) 1544–1552.
[16] E.S. Henson, S.B. Gibson, Surviving cell death through epidermal growth factor (EGF) signal transduction pathways: implications for cancer therapy, Cell. Signal. 18 (2006) 2089–2097.
[17] C. Sutherland, I.A. Leighton, P. Cohen, Inactivation of glycogen synthase kinase-3 beta by phosphorylation: new kinase connections in insulin and growth-factor signalling, Biochem. J. 296 (Pt 1) (1993) 15–19.
[18] J.P.t. Morris, S.C. Wang, M. Hebrok, KRAS, Hedgehog, Wnt and the twisted developmental biology of pancreatic ductal adenocarcinoma, Nat. Rev. Cancer 10 (2010) 683–695.
[19] A. Habiro, S. Tanno, K. Koizumi, T. Izawa, Y. Nakano, M. Osanai, Y. Mizukami, T. Okumura, Y. Kohgo, Involvement of p38 mitogen-activated protein kinase in gemcitabine-induced apoptosis in human pancreatic cancer cells, Biochem. Biophys. Res. Commun. 316 (2004) 71–77.
[20] H. Motoshima, B.J. Goldstein, M. Igata, E. Araki, AMPK and cell proliferation-AMPK as a therapeutic target for atherosclerosis and cancer, J. Physiol. 574 (2006) 63–71.
[21] M. Zakikhani, R. Dowling, I.G. Fantus, N. Sonenberg, M. Pollak, Metformin is an AMP kinase-dependent growth inhibitor for breast cancer cells, Cancer Res. 66 (2006) 10269–10273.
[22] R.J. Dowling, M. Zakikhani, I.G. Fantus, M. Pollak, N. Sonenberg, Metformin inhibits mammalian target of rapamycin-dependent translation initiation in breast cancer cells, Cancer Res. 67 (2007) 10804–10812.

Supplemental Material can be found at:
http://www.jbc.org/content/suppl/2011/08/12/M111.235473.DC1.html

Author's Choice

THE JOURNAL OF BIOLOGICAL CHEMISTRY VOL. 286, NO. 40, pp. 34800–34808, October 7, 2011
© 2011 by The American Society for Biochemistry and Molecular Biology, Inc. Printed in the U.S.A.

L-Tryptophan-mediated Enhancement of Susceptibility to Nonalcoholic Fatty Liver Disease Is Dependent on the Mammalian Target of Rapamycin*[S]

Received for publication, March 1, 2011, and in revised form, August 11, 2011 Published, JBC Papers in Press, August 12, 2011, DOI 10.1074/jbc.M111.235473

Yosuke Osawa[‡§1], Hiromitsu Kanamori[‡], Ekihiro Seki[¶], Masato Hoshi[‡], Hirofumi Ohtaki[‡], Yoichi Yasuda[§], Hiroyasu Ito[‡], Atsushi Suetsugu[§], Masahito Nagaki[§], Hisataka Moriwaki[§], Kuniaki Saito[‖], and Mitsuru Seishima[‡]

From the Departments of [‡]Informative Clinical Medicine and [§]Gastroenterology, Gifu University Graduate School of Medicine, Gifu 501-1194, Japan, the [¶]Department of Medicine, University of California, San Diego, School of Medicine, La Jolla, California 92093, and the [‖]Department of Human Health Science, Graduate School of Medicine and Faculty of Medicine, Kyoto University, Kyoto 606-8507, Japan

Nonalcoholic fatty liver disease is one of the most common liver diseases. L-Tryptophan and its metabolite serotonin are involved in hepatic lipid metabolism and inflammation. However, it is unclear whether L-tryptophan promotes hepatic steatosis. To explore this issue, we examined the role of L-tryptophan in mouse hepatic steatosis by using a high fat and high fructose diet (HFHFD) model. L-Tryptophan treatment in combination with an HFHFD exacerbated hepatic steatosis, expression of HNE-modified proteins, hydroxyproline content, and serum alanine aminotransaminase levels, whereas L-tryptophan alone did not result in these effects. We also found that L-tryptophan treatment increases serum serotonin levels. The introduction of adenoviral aromatic amino acid decarboxylase, which stimulates the serotonin synthesis from L-tryptophan, aggravated hepatic steatosis induced by the HFHFD. The fatty acid-induced accumulation of lipid was further increased by serotonin treatment in cultured hepatocytes. These results suggest that L-tryptophan increases the sensitivity to hepatic steatosis through serotonin production. Furthermore, L-tryptophan treatment, adenoviral AADC introduction, and serotonin treatment induced phosphorylation of the mammalian target of rapamycin (mTOR), and a potent mTOR inhibitor rapamycin attenuated hepatocyte lipid accumulation induced by fatty acid with serotonin. These results suggest the importance of mTOR activation for the exacerbation of hepatic steatosis. In conclusion, L-tryptophan exacerbates hepatic steatosis induced by HFHFD through serotonin-mediated activation of mTOR.

Nonalcoholic fatty liver disease (1) is a component of metabolic syndrome and a spectrum of liver disorders ranging from simple steatosis to nonalcoholic steatohepatitis (NASH),[2] which may cause liver cirrhosis and cancer. Hepatic steatosis occurs when the amount of imported and synthesized lipids exceeds the export or catabolism in hepatocytes. An excess intake of fat or carbohydrate is the main cause of hepatic steatosis. Changes in the dietary nutrient components also modulate hepatic steatosis. Nonalcoholic fatty liver disease patients consume 27% more meat protein from all types of meat (high fat meat, such as beef, liver, sausage, hot dog, and lamb, and low fat meat, such as chicken and turkey), which are sources of dietary tryptophan (2), as well as protein from fish, although less in comparison (3). These reports indicate that hepatic steatosis is also associated with the type of dietary protein consumed in addition to carbohydrate and fat.

Previous studies have shown involvement of amino acids in lipid metabolism in liver. L-Tryptophan is an essential aromatic amino acid and has important roles in protein synthesis and as a precursor of various bioactive compounds, such as serotonin, melatonin, kynurenine, nicotinamide adenine dinucleotide (NAD), and NAD phosphate (NADP). Although L-tryptophan has been widely used as an over-the-counter, natural remedy for depression, pain, insomnia, hyperactivity, and eating disorders (4), various adverse effects of excess tryptophan supplementation have been reported, including fatty liver (2). Oral administration or injection of L-tryptophan induces liver steatosis and increases hepatic fatty acid synthesis in rats (5–7). In mice, the expression of genes associated with the metabolism of L-tryptophan is significantly affected by a high fat diet (8), suggesting the involvement of L-tryptophan in lipid metabolism in the liver. In addition to L-tryptophan itself, its metabolites are also involved in the development of steatosis and steatohepatitis (9, 10).

L-Tryptophan is the precursor in two important metabolic pathways: serotonin synthesis and kynurenine synthesis. Serotonin is synthesized from L-tryptophan by the enzymes tryptophan hydroxylase and aromatic amino acid decarboxylase (AADC), and it regulates physiological functions in the hepatogastrointestinal tract (11). Tryptophan hydroxylase exists in the gastrointestinal tract (12), and AADC exists in the small intestine (13), appendix (13), and liver (14). In a NASH model

* This work was supported by Grants from the Takeda Science Foundation, Mitsubishi Pharma Research Foundation and by Ministry of Education, Culture, Sports, Science, and Technology of Japan Grants 21790657 and 23790787.

[S] The on-line version of this article (available at http://www.jbc.org) contains supplemental Figs. 1–3.

Author's Choice—Final version full access.

[1] To whom correspondence should be addressed: 1-1 Yanagido Gifu, 501-1194, Japan. Tel.: 81-58-230-6430; Fax: 81-58-230-6431; E-mail: osawa-gif@umin.ac.jp.

[2] The abbreviations used are: NASH, nonalcoholic steatohepatitis; AADC, aromatic amino acid decarboxylase; mTOR, mammalian target of rapamycin; HFHFD, high fat and high fructose diet; HNE, 4-hydroxy-2-nonenal; AMPK, AMP-activated protein kinase; ROS, reactive oxygen species; IDO, indoleamine 2,3-dioxygenase; HBSS, Hanks' balanced salt solution.